

# **Development of a 3D printed particle embedded hydrogel mesh for localized delivery of iron-chelating agents**

By

Behnad Chehri Chamchamali

B.Sc., Sharif University of Technology

A Thesis Submitted in Partial Fulfillment of the Requirements for the Degree of

Master of Applied Science

In the Department of Mechanical Engineering

© Behnad Chehri Chamchamali, 2023 University of Victoria

All rights reserved .This thesis may not be reproduced in whole or in part, by photocopying or other means, without the permission of the author.

# **Development of a 3D printed particle embedded hydrogel mesh for localized delivery of iron-chelating agents**

By

**Behnad Chehri Chamchamali**

B.Sc., Sharif University of Technology

## **Supervisory Committee**

---

Dr. Mohsen Akbari, Supervisor (Department of Mechanical Engineering)

---

Dr. Mina Hoorfar, Member (Department of Mechanical Engineering)

# Abstract

By definition, cancer is a disease resulting from uncontrolled growth and division of abnormal cells, which aggregate to form various tumors in neoplasms. Of these neoplasms, glioblastoma (GBM) is one of the most prevalent and lethal type of brain tumor in humans. Only 5% of the patients survive five years after the primary diagnosis. Chemotherapeutics such as temozolomide (TMZ) are used to treat cancer patients with GBM. TMZ is an alkylating agent that can cross the blood-brain barrier (BBB) and minimize the possibility of the disease recurrence. TMZ treatment alone is not sufficient because too much exposure to TMZ causes health issues. Also, It has been shown that cancer cells develop resistance against TMZ. This necessitates using another approach to treat cancer cells. Targeting cancer cells metabolism to inhibit their growth and proliferation could be target of this new approach. Amongst various metabolite contributing in cell, Iron is one of the most necessary component. Iron is crucial for the replication and repair of DNA. Tumor cells often have a greater rate of proliferation than normal cells, which results in a much higher need for iron than that of normal cells. Therefore, removing iron helps in reducing cancer cells proliferation. Iron chelator are compounds that can remove intracellular iron hence induce apoptosis. Deferiprone (DFP) is amongst the most studied anti-cancer drugs with the ability to bypass the BBB and also be used to excrete the excess iron form the body. However, prolonged oral administration of this drug can be dangerous, which causes common side effects such as nausea, vomiting, infections. This brings up the need for a new method of drug delivery which leads to the usage of localized drug delivery systems. Due to the fact that, such techniques help to increase drug absorption at the tumor site and help reduce the dosage frequency and minimize side effects. Compared to systemic administration, local delivery to GBM includes several benefits such as avoiding the BBB and enhancing the local therapeutic bioavailability. As a result, much effort has been expended in developing novel therapeutic approaches capable of delivering an anticancer medication at the tumor site. This covers system architectures

such as wafers, microspheres, CED, hydrogels and meshes. Microspheres constructed of biodegradable polymers have the ability to maintain the chemotherapeutic agent intact within the carrier and administer the medicine locally for a longer length of time whilst helping nutrients to still be delivered to the desired area with minimal obstructions. The use of polymeric particles may be challenging since the highlighted particles are transferred around the tissues and hence dislodge from their designated surface areas. Therefore, the use of a hydrogel based mesh is introduced. Alginate is a naturally occurring hydrogel, which is appropriate for three-dimensional scaffolding materials. Alginate as a mesh substrate included desirable characteristics such as versatile characteristics with the placement of the mesh as well as prevention of the particles from transferring and dislocating inside the cerebral spinal fluid.

In this thesis, two major methods of microparticle fabrication were used. Due to the nature of TMZ and DFP, oil-in-oil single emulsion and water-in-oil-in-water double emulsion were used in this study, respectively, to create PLGA based microparticles. After particle fabrication, they were embedded inside an alginate mesh substrate created using a 3D printer whilst implementing an extrusion-based 3D printing method, which provides the benefit of stationary particles. The resulting mesh was then placed in specific control media to measure the release of TMZ and DFP throughout the process. The data shown here depicts great potential in the use of a hydrogel-based particle embedded mesh for the deliverance of iron-alkylating agents.

# Contents

<b>Supervisory Committee.....</b>	<b>ii</b>
<b>Abstract .....</b>	<b>iii</b>
<b>Contents.....</b>	<b>v</b>
<b>List of Tables.....</b>	<b>vii</b>
<b>List of Figures .....</b>	<b>viii</b>
<b>List of Abbreviation .....</b>	<b>10</b>
<b>Acknowledgments.....</b>	<b>12</b>
<b>Dedication .....</b>	<b>13</b>
<b>Chapter 1.....</b>	<b>1</b>
<b>Introduction .....</b>	<b>1</b>
1.1 Treatment strategies for GBM.....	5
1.1.1 Surgery.....	5
1.1.2 Radiotherapy .....	6
1.1.3 Chemotherapy .....	7
1.1.4 Immunotherapy .....	7
1.2 Combination therapy for GBM treatment.....	8
1.2.1 Combination of chemo and radiotherapies.....	9
1.2.2 Combination of chemo and immunotherapies.....	10
1.2.3 Combination of multiple immunotherapies .....	11
1.2.4 Chemotherapy with use of Iron chelating agents .....	11
1.3 Localized therapy strategies for GBM treatment .....	14
1.3.1 Prolonged drug delivery eluting wafers .....	14
1.3.2 Drug-eluting Particles.....	15
1.3.3 Polymeric microspheres.....	16
1.3.4 Convection-enhanced drug delivery systems .....	18
1.3.5 Hydrogels.....	20
1.3.6 Mesh.....	20
1.4 Conclusion.....	21
<b>Chapter 2 .....</b>	<b>24</b>

<b>Production of polymer-based microparticles.....</b>	<b>24</b>
2.1 Materials and Methods.....	27
2.1.1 Preparation of DFP encapsulated microparticles.....	27
2.1.2 TMZ microparticles.....	28
2.2 Results and Discussion .....	30
2.2.1 DFP microparticles .....	30
2.2.2 TMZ microparticles .....	38
2.3 Conclusion.....	40
<b>Chapter 3 .....</b>	<b>41</b>
<b>Fabrication of alginate mesh .....</b>	<b>41</b>
3.1 Materials and Methods.....	43
3.1.1 Fabrication of the alginate scaffold .....	43
3.1.2 Fabrication of DFP microparticle loaded alginate mesh .....	44
3.1.3 <i>In vitro</i> release of DFP particles.....	45
3.2 results and Discussion .....	46
3.3 Conclusions .....	50
<b>Chapter 4 .....</b>	<b>51</b>
<b>Conclusion and Future work .....</b>	<b>51</b>
<b>Appendix A.....</b>	<b>54</b>
<b>Additional Information .....</b>	<b>54</b>
<b>Bibliography.....</b>	<b>56</b>

# List of Tables

**Table 1.1** Overview previous work done PLGA particles ..... 18

**Table 2.1** Overview of DFP and TMZ-loaded microparticles using various methods of fabrication based on their encapsulation efficiencies ..... 31

# List of Figures

<b>Figure 1.1</b> Overview of GBM survival rates depending on age; reproduced with permission [Thakkar et al., 2014].....	3
<b>Figure 1.2</b> Various pathways of GBM formation reproduced with permission [courtesy of Ohgaki and Kleihues, 2012].....	3
<b>Figure 1.3</b> Anatomy of blood brain barrier [reproduced with permission [Lawther et al., 2011]].....	4
<b>Figure 1.4</b> Overview of iron-chelating agents in clinical use; reproduced with permission [Massachusetts Medical Society (Asija et al., 2022)].....	12
<b>Figure 1.5</b> Implanted BCNU-loaded glial wafers inside the brain; reproduced with permission from [Wolinsky et al., 2012].....	15
<b>Figure 1.6</b> CED use inside the anatomy of the brain; reproduced with permission [Mehta et al., 2017].....	19
<b>Figure 1.7</b> Overview of various methods for fiber-based scaffold fabrication; reproduced with permission [Tamayol et al., 2013].....	21
<b>Figure 2.1</b> The hydrolysis mechanism of PLGA.....	26
<b>Figure 2.2</b> SEM micrographs of various synthesized microparticles. First row, left to right, DFP encapsulated PLGA particles using w/o/w method at respectively 5, 10 and 15% PLGA; second row, TMZ encapsulated PLGA particles using o/o method at respectively 5, 10 and 15% PLGA.....	32
<b>Figure 2.3</b> Overview of various release profiles of DFP for various PLGA concentrations in ACSF.....	33
<b>Figure 2.4</b> Overview of various release profiles of DFP for various PLGA concentrations in DMEM.....	34
<b>Figure 2.5</b> Overview of various release profiles of DFP for various PLGA concentrations in ACSF.....	35
<b>Figure 2.6</b> Overview of various release profiles of DFP based on various PLGA concentrations in DMEM.....	35
<b>Figure 2.7</b> Overview of various release profiles of DFP based on 5% PLGA concentration and fabrication methods in DMEM and ACSF.....	36
<b>Figure 2.8</b> Overview of various release profiles of DFP based on 10% PLGA concentration and fabrication methods in DMEM and ACSF.....	37

<b>Figure 2.9</b> Overview of various release profiles of DFP based on 15% PLGA concentration and fabrication methods in DMEM and ACSF .....	38
<b>Figure 2.10</b> Overview of various release profiles of TMZ based on various PLGA concentrations in ACSF and DMEM the top and bottom graph respectively .....	39
<b>Figure 3.1</b> Process of 3D printing a hydrogel from start to post fabrication crosslinking; reproduced with permission [Urruela-Barrios et al., 2019].....	42
<b>Figure 3.2</b> Alginate hydrogel formation using calcium; reproduced with permission [Bonilla et al., 2018] .....	42
<b>Figure 3.3</b> Image of the commercial 3D bioprinter CELLINK and the single-needle extrusion technology used to prepare both blank and with microsphere-loaded meshes.....	43
<b>Figure 3.4</b> Image of double-syringe method for mixing particles and alginate hydrogel .....	44
<b>Figure 3.5</b> Images of the GlioMesh post printing and crosslinking .....	46
<b>Figure 3.6</b> Micrographs of alginate meshes printed using various pressures (80, 120 and 160 kPa).....	47
<b>Figure 3.7</b> Micrographs of alginate meshes printed using various printing speeds (150, 250 and 350 mm/min).....	47
<b>Figure 3.8</b> Micrographs of alginate meshes printed using various particle concentrations (1,3 and 6 mg/ml) .....	48
<b>Figure 3.9</b> Cumulative releases of DFP encapsulated microparticles embedded in alginate meshes .....	49

# List of Abbreviation

ACSF = Artificial cerebrospinal fluid

Alginate function = A common role of alginates in pharmacy is as a thickener gelling agent and stabilizer. Alginate can play significant role in controlled release drugs

BBB = Blood-brain barrier

CNS = Central nervous system

CT = Computerized tomography

DFP = Deferiprone (DFP) is an oral iron-chelating agent used to treat transfusion-related, chronic iron overload

DMEM = Dulbecco's modified Eagle medium

Double emulsion method = A novel method of dissolving a drug in an aqueous solution and further emulsifying it in a molten lipid

Hydrogels = Used for three purposes in tissue engineering and serve as interstitial fillers, as carriers for the delivery of bioactive molecules and scaffolds for the cells. Moreover, hydrogels can be used as 3D structures to help form ideal tissues.

Microparticles function = Can be used to encapsulate nanoparticle systems and polymers such as chitosan can be used to improve mucoadhesive characteristics and maintain drug delivery

Microspheres = Spherical microparticles used, where consistent and predictable particle surfaces are important

MRI = Magnetic resonance imaging

O/O = Oil-in-Oil

O/W = Oil-in-Water

OS = Prolong Overall Survival

PFS = Progression-free survival

PLGA polyester = It is a copolymer of polylactic acid (PLA) and polyglycolic acid (PGA). In terms of design and performance, it is the most well-defined biomaterial that can be used for drug delivery.

SEM = Scanning electron microscopy

Single emulsion method = Allows modification of various formulation parameters, each of which can modify characteristics of the nanoparticles

TMZ = Temozolomide (TMZ) is an alkylating chemotherapy key agent for the glioblastoma treatment

W/O/W = Water-in-oil-in-water

# Acknowledgments

I would like to thank:

My supervisor, Dr. Mohsen Akbari, for his mentoring, support, encouragement and patience throughout my time at the university.

Furthermore, I would like to thank Dr. Amir Seyfour, Dr. Meitham Amerah, Dr. Mahmood Razzaghi, Evan Stefanek and Dr. Golnaz Vaseghi for their help and support within my time at the university.

## **Dedication**

I dedicate this thesis to my lovely mother and father. Without their kind support (in the best and worst moments of my life), I would never have been able to achieve what I have.

# Chapter 1

## Introduction

By definition, a brain tumor is a cluster of abnormal cells allocated inside the brain tissue. This can cause numerous health issues such as headaches, seizures, chronic nausea, vomiting and fatigue as well as mental or behavioral abnormalities such as memory issues or personality changes, gradual weakening or paralysis on one side of the body and visual or speech impairments and death. A tumor is classified into two major categories primary and secondary [Woodworth et al., 2014]. Primary brain tumors are a class of tumors that originate from the brain [Germano et al., 2010]. In contrast, secondary tumors originate from other parts of the body, move toward the brain and form a tumor [Woodworth et al., 2014]. Brain tumors are classified based on how quickly they develop and how likely they return following therapy. With the current knowledge of medicine, the World Health Organization (WHO) has hierarchically classified all known tumors into four major classifications [Jawhari et al., 2016]. Tumors in Grades I and II are addressed as low grades, whereas tumors in Grades III and IV are highlighted as high grades. Most of all glial tumors are made up of Grade IV glioma [Mesfin & Al-Dhahir, 2017]. Many genetic and environmental variables in glioblastoma multiforme have been investigated; however, no risk factors that account for a significant proportion of the glioblastoma (GBM) incidence has been discovered [Kanderi & Gupta, 2021]. Studies have shown a direct line of causality between GBM patients and their ages [Jovcevska, 2019]. This corresponds with the fact that by increasing the age, the proportion of total recovery decreases.

The average yearly age-adjusted incidence rate (IR) of GBM is 3.19/100,000 people, based on 2013 CBTRUS (Central Brain Tumor Registry of the United States) study. This is the malignant brain and CNS tumor with the greatest IR. The median age of GBM diagnoses is 64 years in adults. The disease incidence increases with age, reaching a peak between

the ages of 75 and 84 and then decreasing after the age of 85 [Kanderi & Gupta, 2021]. Reportedly, this type of tumor is rarely seen in youths in the community [Thakkar et al., 2014]. One of the biggest reasons for a low survival rate (Figure 1.1) with various types of therapy such as surgery in the elderly community is associated with the body response post-therapy on if the body tolerates the aftermath [Thakkar et al., 2014]. Glioblastoma is the adults' most common and aggressive primary malignant brain tumor and constitutes over 90% of all tumors [Bausart et al., 2022]. Studies of this tumor have shown that primary and secondary GBMs have similar morphologies but the factor that separates them is their development through various processes [Figure 1.2] [Jawhari et al., 2016].

Technically, GBM has thus been shown to be resistant to traditional and cutting-edge targeted therapies [Fabro et al., 2022]. Despite advancements in medicine, especially in neuro-oncology, GBM treatment is still difficult [Combs et al., 2008] with a low success rate of complete tumor removal without complications or damaging healthy tissues around it [Stewart and Burdett, 2002]. Based on studies in recent years, surgery only improves the patients' lifespan by half a year [Wilson et al., 2014]. With post-surgery treatments, this can be extended to almost a year and is as effective as post-surgery using conventional combination therapy of chemotherapy and radiotherapy [Stupp et al., 2005]. There are several factors contributing to the effectiveness of drugs. The most effective factor includes the blood brain barrier (BBB) (Figure 1.3), composed of tight junctions joined with endothelial cells that significantly decrease the effectiveness of the drugs [Ananta et al., 2016] [Wohlfart et al., 2012]. Currently, Temozolomide (TMZ) is one of the best drugs in chemotherapy due to its nature of passing through the BBB. Despite the fact that TMZ is the most used drug in chemotherapies, its short lifespan makes it hard to administer the drug with effective doses, which leads to systematic administration [Ananta et al., 2016].

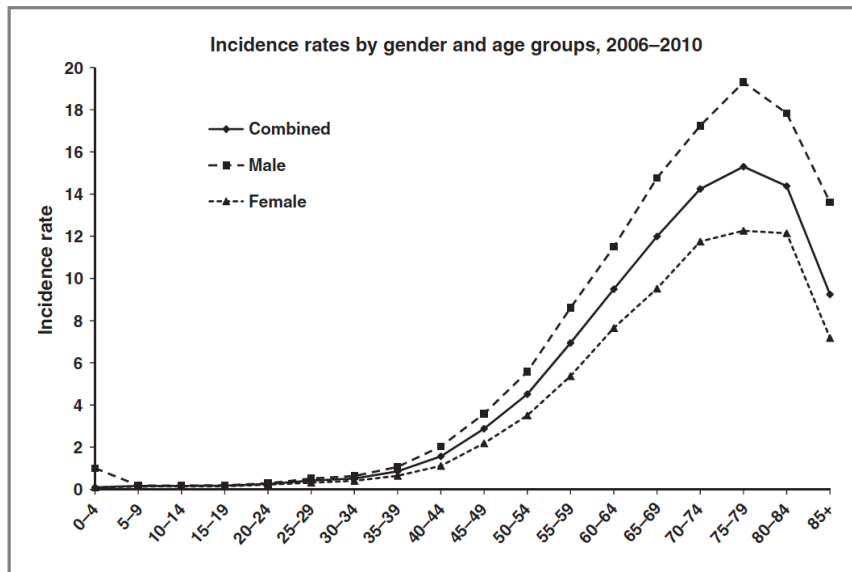


**Figure 1.1** Overview of GBM survival rates depending on age; reproduced with permission [Thakkar et al., 2014]

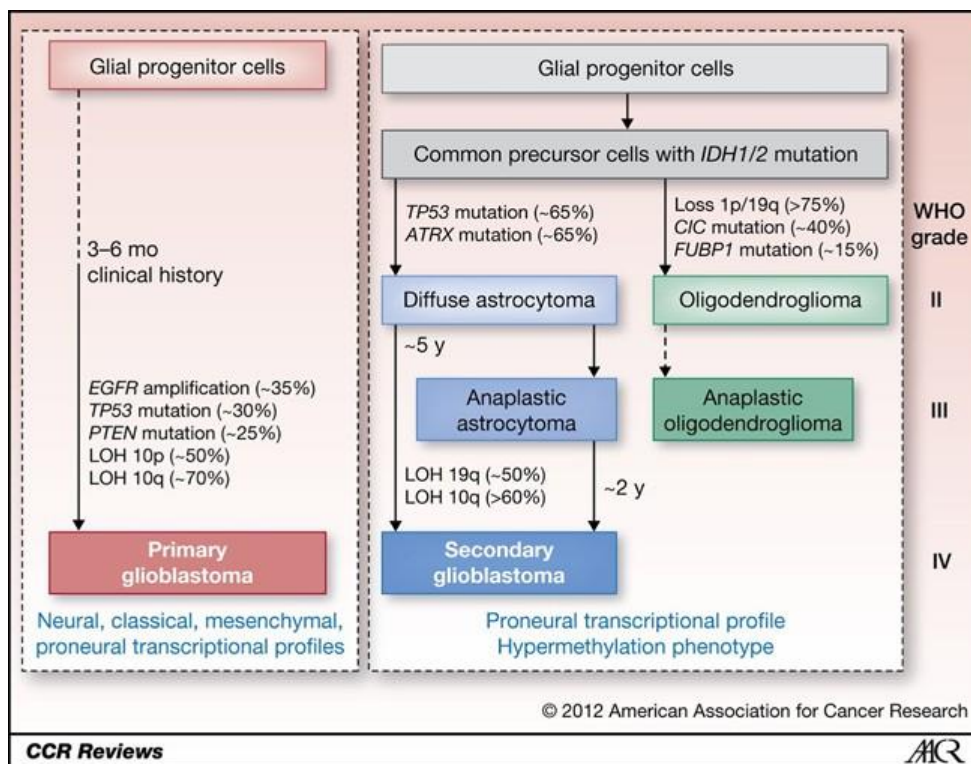


**Figure 1.2** Various pathways of GBM formation reproduced with permission [courtesy of Ohgaki and Kleihues, 2012]

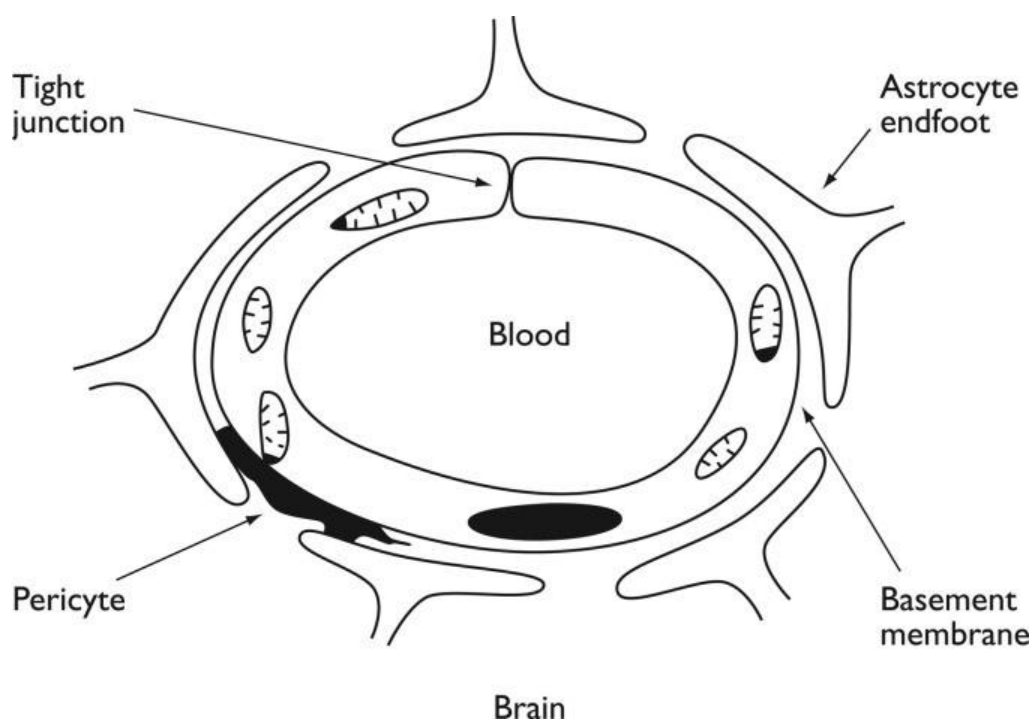


**Figure 1.3** Anatomy of blood brain barrier [reproduced with permission [Lawther et al., 2011]]

Administration of the prolonged oral drug causes side effects in GBM patients, including nausea, headache, fatigue and sometime serious effects in bone marrow [Ananta et al., 2016]. Although there are several strategies for battling GBM, the success rate is very low in almost all of them, with the recurrence of GBM tumors in various sites [Guerin et al., 2004]. To increase effectiveness of the medicines, it is critical to create resistance-fighting tactics. Finding the most effective method to combat medication resistance is particularly difficult due to the significant genetic variability in cancers and intricacy of tumor development. Therefore, the first step in solving this problem is to comprehend the underlying reasons for the resistance. The first critical step to further correctly anticipate clinical behaviors and medication responses, including resistance, includes creation of *in vitro* models that faithfully recreate the biology of GBM [Fabro et al., 2022]. This thesis has focused on developing a novel treatment strategy of using microparticle-loaded 3D-printed drug-eluting mesh capable of releasing DFP and TMZ in Unison and prolonged state to decrease the recurrence of the tumors and increase effectiveness of the drugs.

## **1.1 Treatment strategies for GBM**

One of the most prevalent, deadly, aggressive primary astrocytoma types with a dismal prognosis is GBM multiforme [Aldoghachi et al., 2022]. With 14.5% of all central nervous system (CNS) tumors and 48.6% of malignant CNS tumors, GBM multiforme is one of the most aggressive cancers. Patients with GBM have a 15-month median overall survival (OS) [Grochans et al., 2022]. Traditional treatment modalities, including surgery, radiation and chemotherapy, have been incorporated as part of routine therapies during the past 20 years. Currently, radiation treatment is used in combination with chemotherapy and temozolomide after surgical tumor removal [Aldoghachi et al., 2022]. Together, these intensive treatment methods have offered tolerable levels of toxicity with minor survival benefits. However, relapse invariably occurs and always results in mortality in the vast majority of patients. Relapse can occur for a variety of reasons, including medication resistance, immunosuppressive tumor microenvironment, stemness of glioma cells, tumor heterogeneity and increased hypoxia and angiogenic factors. Therefore, development of novel therapeutic strategies is urgently needed to treat GBM [Asija et al., 2022].

### **1.1.1 Surgery**

Before treatment of GBM begins, the initial step must include surgery [Omuro and DeAngelis, 2013]. This technique has several benefits, one of them being the decrease of tumor tissues and providing valuable tissues for study [Hou et al., 2006]. Before surgery, the major point is to locate the tumor; hence, Magnetic resonance imaging (MRI) scans and computerized tomography (CT/CAT) scans are used. Surgery in malignant gliomas helps prolong overall survival (OS) and progression-free survival (PFS), acquisition of histopathological and molecular information and decrease use of steroids owing to the reduction of mass effect. However, for a long time, significant resection in the elderly people was avoided for fear of poorer

results. Recent studies have emphasized the need and safety of intensive surgical therapy, especially in elderly people [Klingenschmid et al., 2022]. Although surgery is the first option in cancer treatment, doing surgery to completely remove the tumor is not suggested as it may include unnecessary complications and serious neurological damage to the surrounding areas [Jadhav et al., 2007]. Due to the aggressive nature of GBM, complete removal is almost impossible [Adamson et al., 2009].

### **1.1.2 Radiotherapy**

Surgery is the initial step for GBM treatment and a post-surgery therapy for GBM is radiotherapy [Fernandes et al., 2017]. Studies have shown that the survival rate for GBM patients has doubled through the treatment [Poon et al., 2020]. Radiotherapy is an appropriate strategy because patients are exposed to radiation to kill GBM cells remaining in the brain after surgery [Wee, 2022]. However, effectiveness and dosage are highly dependent on the patients. Patients' organ sensitivity such as the frontal lobe determines the effectiveness of radiotherapy and limits the dosage [Nazemi-Gelyan, 2015]. Although radiotherapy has been verified as an effective strategy, complete exposure of the brain to radiation is hazardous as radiation damages the brain, in contrast to fractional focal radiation therapy [Turnquist, Harris, & Harris, 2020]. In recent studies, it has been reported that fractional therapy is a viable option similar to whole-brain therapy, if not better [Chao et al., 2001]. Fractional focal radiotherapy, typically used for patients, usually includes the administration of a 2Gy dose over a 5-day time period [Adamson et al., 2009]. Although radiotherapy does not pose immediate risks, the addition of improved survival rates makes GBM cells become resistant due to their nature of hypoxia [Flynn et al., 2008]. The current standard of treatment for adults with newly diagnosed GBM, who are under 70 years old in excellent general and neurological health and who receive radiotherapy in addition to concurrent and adjuvant TMZ chemotherapy (the "Stupp protocol") [Abbruzzese et al., 2022].

### **1.1.3 Chemotherapy**

The most widely used method of treatment for GBM is chemotherapy [Wiwachitawee et al., 2021]. Chemotherapy is a method that can be used simultaneously with other methods or as a unique option for cancer treatment [Mokhtari et al., 2017]. A well-known method to sensitize the brain to the effects of radiotherapy is to use chemo-radio sensitization [Citrin & Mitchell, 2014]. This method has been shown to significantly improve the available treatments as chemotherapy is prescribed with radiotherapy after surgery in Unison. However, there are still negative effects that need to be considered. The most important negative effect includes the fact that patients are still prescribed toxic drugs for prolonged periods even after surgery, which leads to the decreased general health of the patients. A majority of trials have been carried out on TMZ chemotherapy combined with radiotherapy or standard chemotherapy based on nitrosoureas and radiotherapy. A novel oral alkylating drug called TMZ, for example, has been reported to have anticancer efficacy when used to treat newly discovered malignant gliomas. Chemotherapy, radiation and surgical resection are currently the mainstays of treatment for newly diagnosed GBM. Effectiveness of the chemotherapy, whether administered as a pre-radiotherapy step or an adjuvant, is still debatable [Wang et al., 2017].

### **1.1.4 Immunotherapy**

The human body includes a defense line called the immune system. This immune system acts harmonically and includes costimulatory signals and inhibitors [Sharpe, 2009]. To control the immune system, the body has created specific immune checkpoints that regulate the immune system. These regulating checkpoints help provide the body with modified immune responses, preventing autoimmunity [Li et al., 2018]. Since advancements

in this field have direct correlations with other treatment strategies, one of which is immunotherapy [Funes et al., 2019]. The purpose of immunotherapy is to boost the immune system of the body to recognize GBM cells and attack and destroy them [Pearson et al., 2020]. Moreover, immunotherapy develops memory cells to stop the GBM cells from reproducing and prevent GBM recurrence [Asija et al., 2022]. Immunotherapy helps decrease growth of this aggressive cancer in combination with other treatment modalities, including radiation and laser therapy. Another potential immunotherapy strategy includes antitumor vaccines. By boosting adaptive immune system through vaccination, the protocol encourages successful therapeutic responses to GBM. While immunotherapy for GBM includes numerous challenges, it offers much room for development. Immunotherapy for GBM includes a variety of challenges. The BBB could be the greatest impediment as it maintains biological processes stable and protects cells against toxication and microbial invasion of the CNS [Chowdhury et al., 2021].

## **1.2 Combination therapy for GBM treatment**

With all the methods for the treatment of GBM, there are still hindrances that can affect them, including a variety of obstructions that make the highlighted therapies lose their efficacy. A major obstruction is the BBB. Four major factors contribute to the efficacy of drugs, including (1) BBB, (2) the tumor microenvironment, (3) heterogeneity and (4) angiogenesis [Asija et al., 2022]. The brain is governing the body. The brain is an immune-privileged site meaning that it can tolerate foreign implementations such as antigens without inflammatory responses. The BBB is composed of three subsequent layers of (1) glycocalyx, (2) endothelium and (3) extravascular [Asija et al., 2022]. The BBB does not have a fixed geometry; hence, it can exist in the body with various shapes and sizes. This is extremely important because the occurrence of a tumor has direct effects on BBB structure integrity leading the tumor recurrence.

The Discovery of glioma stem cells resulted from research by Singh et al, revealing their existence in the tumor microenvironment [Asija et al., 2022]. This microenvironment consists of a variety of parts, which all lead to the behavior of GBM and its high tolerance to regular GBM treatment therapies. The behavior of these glioma stem cells is almost identical to healthy stem cells. These glioma stem cells are the major causes of tumor initiation, cell migration and invasion [Vollmann-Zwerenz et al., 2020]. These characteristics of the glioma cells make treatments such as chemotherapy and immunotherapy and various drugs have low efficacies with almost always recurrence of GBM [Auffinger et al., 2015]. Tumor characteristics majorly depend on their molecular and cellular heterogeneity structures that define its aggressiveness as well as its reluctance to anticancer drugs [Diaz-Cano, 2012]. The specific attribute of the heterogeneity of GBM cells includes a great problem with the present GBM treatment options [Asija et al., 2022]. Hypoxia is a term widely used in the field of cell studies. This is a state in which the level of oxygen in the environment is lower than what is needed. This leads to corruption in the nutrient stream to the cells, formation of abnormalities and genetic changes. Furthermore, hypoxia is the controlling factor of angiogenesis in tumor microenvironments. Finally, hypoxia and angiogenesis cooperate with each other and create immunosuppressive environments [Asija et al., 2022]. Over the past decades, great advancements have occurred in science, which has led to newer and great accomplishments. However, the current problem is that novel innovative treatment strategies are needed for GBM. These have led to the use of various treatment strategies in Unison to meet the necessary criteria [Asija et al., 2022].

### **1.2.1      Combination of chemo and radiotherapies**

Nowadays, a variety of treatment strategies are used for GBM treatment [El-Khayat & Arafat, 2021]. Of these strategies, radiotherapy in combination with chemotherapy with TMZ is one of the most used options

that are available [Parisi et al., 2015]. One of the major reasons that this treatment strategy is commonly used is that TMZ is an alkalinizing agent [Strobel et al., 2019]. This specific treatment option is unique due to its nature that helps increase toxicity levels and apoptosis O6-methylguanine (O6-MeG), which is a toxic element that can be eradicated and broken down by the body enzymes called O6-methylguanine-DNA methyltransferase (MGMT) [Fan et al., 2013]. These enzymes help rewind damages that are induced in cells with the removal of O6-methylguanine (O6-MeG). This inevitably results in cell survival [Asija et al., 2022]. The current standard of care for GBM includes safe maximum tumor resection, followed by concurrent radiation and TMZ chemotherapy (75 mg/m<sup>2</sup>/day for 6 w) (60 Gy in 30 fractions) [Lara-Velazquez et al., 2021].

### **1.2.2 Combination of chemo and immunotherapies**

One of the most extensively studied treatment therapies for GBM is the combination of immunotherapy and chemotherapy, especially with TMZ [Bausart et al., 2022]. As previously stated, the immune checkpoint blockade is greatly important as it can improve or break the efficacy of the treatments. A combination of chemotherapy with TMZ and immunotherapy with ICB is effective in recognizing and destroying cancerous cells [Bausart et al., 2022]. Furthermore, the use of TMZ helps therapists achieve first-response protocols for the body such as first-line anti-tumor immune responses [Candolfi et al., 2014]. Although TMZ has been verified as a cognitive part of chemotherapy and cancer treatment, the dosage of TMZ is a fine line that should be tread carefully. Small doses decrease efficacy while large doses increase lymphopenia and T-cell exhaustion [Bausart et al., 2022].

### **1.2.3 Combination of multiple immunotherapies**

Nowadays, there is no Food and Drug Administration (FDA) approved immunotherapies for GBM to help relieve cancer patients [Bausart et al., 2022]. Over the past years, immunotherapy has undergone a variety of studies; however, a vast majority of the studies are focused on the assessment of toxicity in the body. Although immunotherapies have merited this as a standalone procedure for the treatment in Unison or as a supplementary method to those already available [Vanneman & Dranoff, 2012]. Although combination therapies might be the future of treatment, there are still many unknown issues [Krishnareddy & Swaminath, 2014]. The current lack of information prevents further rapid advancements [Bausart et al., 2022].

### **1.2.4 Chemotherapy with use of Iron chelating agents**

For the appropriate functioning of several cellular processes, including DNA synthesis and cell cycle progression, iron is a necessary component [Heath et al., 2013]. Because there are no efficient ways for human cells to eject extra iron, long-term blood transfusions inevitably lead to the clinical complications of iron overload [Rasel & Mahboobi, 2022]. Iron-induced liver diseases and endocrine abnormalities occur during childhood in  $\beta$ -thalassemia patients, who receive blood transfusions from infancy and the following mortality from iron-induced cardiomyopathy usually occurs in adolescence [Pinto & Forni, 2020]. Behaviors of the transfused red blood cells (RBCs) change when they are close to the end of their lifespan [Sparrow, 2010].

Variable	Deferoxamine	Deferasirox	Deferiprone
Chelator-iron complex	Hexadentate, 1:1 complex	Tridentate, 2:1 complex	Bidentate, 3:1 complex
Usual dose	25–50 mg/kg/day	20–40 mg/kg/day	75–100 mg/kg/day
Administration	Subcutaneous or intravenous, 8–10 hr/day, 5–7 days/wk	Oral, once daily	Oral, three times daily
Plasma half-life	20–30 min	8–16 hr	2–3 hr
Route of elimination	Biliary and urinary	Predominantly biliary	Predominantly urinary
Regulatory approval	Approved in United States, Canada, Europe, and other countries	Approved in United States, Canada, Europe, and other countries	Not approved in United States or Canada; approved in Europe <sup>11</sup> and other countries
Indication	Transfusional iron overload	Transfusional iron overload	Transfusional iron overload in patients with thalassemia major, when deferoxamine therapy is contraindicated or inadequate
Adverse effects	Irritation at the infusion site, ocular and auditory disturbances, growth retardation and skeletal changes, allergy, respiratory distress syndrome with higher-than-recommended doses <sup>12</sup>	Gastrointestinal disturbances, rash, increase in serum creatinine level; potentially fatal renal and hepatic impairment or failure, gastrointestinal hemorrhage <sup>13</sup>	Agranulocytosis and neutropenia; gastrointestinal disturbances, arthropathy, increased liver-enzyme levels, low plasma zinc level, progression of hepatic fibrosis associated with increase in iron overload or hepatitis C <sup>11</sup>

**Figure 1.4** Overview of iron-chelating agents in clinical use; reproduced with permission [Massachusetts Medical Society (Asija et al., 2022)]

Hemoglobin of these RBCs is digested and hence iron from the RBC heme is stored and then dispersed within the cytosol and stored inside reticuloendothelial macrophages [Korolnek & Hamza, 2015]. Macrophages and hepatocytes can no longer store the extra iron with repeated blood transfusions. Then, iron enters the plasma more than the circulating transferrin can handle. Thus, non-transferrin-bound iron appears in the plasma as a heterogeneous collection of iron complexes that seems to be the primary mediators of extrahepatic tissue damages in transfusion iron overloads. With these limitations, therapies with the use of iron-chelating agents have become further popular (Figure 1.4) [Mobarra et al., 2016]. These iron-chelating agents start to form complexes with the existing iron that help improve the removal of excess iron through natural mechanisms. Of these iron chelators, there are three specific drugs that are used for GBM treatments [Valdés et al., 2010]. Deferasirox (DFX) and deferoxamine (DFO) are iron chelators currently approved for use in the United States and Canada with a third synthetic oral agent of deferiprone (DFP), which is approved to be used in the European Union countries as well as other

countries [Entezari et al., 2022]. From these iron chelators, TMZ is important. TMZ is a prodrug of the anti-cancer medication, Temodar, and an imidazotetrazine derivative of the alkylating agent, dacarbazine [Asija et al., 2022].

Iron is essential for proteins and enzymes that control respiratory complexes, DNA and heme productions, mitosis, and epigenetic alterations in non-cancerous cells. However, all of these functions are dysregulated in cancer [Lane et al., 2014]. Iron insufficiency inhibits activity of iron-requiring enzymes in tissues; nevertheless, excessive iron accumulation causes toxicity by activating cell death signaling pathways via oxidative stress [Xie et al., 2016]. To maintain appropriate safe iron levels, cells express wide ranges of proteins that carefully control intracellular and systemic iron metabolisms [Rouault, 2006]. Iron in the systemic iron pools is often linked to transferrin (TF). The iron-loaded TF then forms a complex on the cell plasma membrane (PM) with transferrin receptor 1 (TfR-1), which is absorbed through endocytosis [Hentze et al., 2010]. Cancer cells use several other routes for maintaining cellular iron balances. The epidermal growth factor receptor (EGFR) has been shown to affect iron metabolism in non-small-cell lung cancer cells (NSCLC) by directly binding and redistributing TfR-1. Technically, TfR-1 on the cellular surface decreases by EGFR inactivation, resulting in decreased iron import and cell cycle arrest [Zhang et al., 2015]. Free non-bound iron molecules cause deadly cellular toxicity, triggering iron-dependent non-apoptotic cell death that is commonly known as ferroptosis if intracellular iron homeostasis is not strictly maintained in cancer cells [Dixon et al., 2012]. Therefore, ferroptosis targeting may include therapeutic promises for a variety of recurrent mesenchymal (MES) cancers such as GBM [Bao et al., 2021]. Most anticancer medicines targeting the elimination of iron by chelation are unlikely to be cancer tissue-specific, particularly in the iron-dependent brain. Therefore, targeting iron control within tumor-specific and/or overactive pathways suggests a viable strategy for disabling critical cancer reliance [Schonberg et al., 2015]. Furthermore, in several drug-resistant MES-type malignancies, increased iron intake may result in cellular

susceptibility to ferroptosis, which receives further attentions as a therapeutic target [Viswanathan et al., 2017]. In a 2022 study, researchers detailed iron commensalism of MES GSCs (GBM stem cells) in mixed GBM tumors and addressed ferroptosis as a possible therapy for aggressive GBM by targeting symbiosis of PN and MES subtypes [Vo et al., 2022].

### **1.3 Localized therapy strategies for GBM treatment**

#### **1.3.1 Prolonged drug delivery eluting wafers**

Based on the studies, patients diagnosed with GBM have a mean life expectancy of nearly a year even with the use of the three treatment methods previously highlighted [Hanif et al., 2017]. Thus, a novel treatment strategy is needed for the prolonged introduction of chemotherapy drugs at high doses. The FDA has therefore suggested the use of Gliadel® wafers in addition to standard treatments. This method is used as a supplementary method or an initial response to GBM [Guerin et al., 2004]. This biodegradable polymer-based drug delivery system is composed of 3.85% BCNU in poly-[bis-p-(carboxyphenoxy)propane-sebacic acid] copolymer (PCPP-SA). These wafers are manufactured into eight individual pieces with similar sizes of roughly 20 mm and secured in their places using blood clot-inducing material called Surgical [Guerin et al., 2004]. The wafers are used to control the release of BCNU to the desired areas within a few weeks. Although the use of wafers provides significant advantages, there are still drawbacks [Woodworth et al., 2014]. First, wafer morphology cannot be used in every situation. Moreover, wafers are almost rigid. They are not able to completely cover the infected areas, which materializes itself into a nonuniform distribution of BCNU [Woodworth et al., 2014]. Second, this method is only viable for unilateral tumors. Third, because of prolonged drug diffusion can lead to numerous health complications such as nausea, headaches and other complications, which directly affect the patients' health [Guerin et al., 2004].



**Figure 1.5** Implanted BCNU-loaded gliadel wafers inside the brain; reproduced with permission from [Wolinsky et al., 2012]

### **1.3.2 Drug-eluting Particles**

With Gliadel wafers, the size of the wafers is a crucial factor in efficiency of the treatment [Xing et al., 2015]. Thus, an alternative method is suggested that still can deliver a certain quantity of BCNU to the affected areas and bypass the BBB [S Hersh, 2016]. Particles were introduced for this mean. Particles loaded with similar chemotherapy drugs can provide an appropriate replacement for the wafers as they do not need invasive surgeries [Gil-Alegre et al., 2008]. Poly(D, L-lactide-co-glycolide) (PLGA) is a well-known biocompatible and biodegradable polymer approved by the US FDA for medical uses [Makadia & Siegel, 2011]. Encapsulated therapeutic agents within the microspheres are generally released through diffusion, erosion mechanisms, or a combination of the two mechanisms [Ananta et al., 2016]. Moreover, the hydrophobic nature of the particles causes limited interactions between the drugs and their surrounding aqueous phase [Sarkar & Kellogg, 2010]. Despite the good characteristics of the particles, other characteristics must be considered. For example, encapsulation efficiency plays significant roles in the efficacy of the

particles [Ananta et al., 2016]. Due to the direct introduction of particles into the brain, complications may occur with no efficient ways of controlling the particles. This means that particles shift, and the efficacy of the drug is affected because of the flow of cerebral fluid in the brain [Menei et al., 1993].

### **1.3.3 Polymeric microspheres**

Wafer-like treatments for GBM patients can be replaced by polymer-based microspheres that contain chemotherapeutic medicines. Because microspheres are much smaller, intrusive operations are no longer necessary [Gil-Alegre et al., 2008]. A well-known biocompatible and biodegradable polymer authorized for use in medical use by the US Food and Drug Administration (FDA) is poly(D,L-lactide-co-glycolide) (PLGA) [Ananta et al., 2016]. Biodegradation of PLGA-made microspheres eliminates the need for surgical removal of the implanted carriers following therapy [Menei et al., 1993]. Additionally, the greater hydrophobicity of PLGA prevents the integrated agent from interacting with the surrounding aqueous environment, preserving the medicine intact inside the carrier [Wu, 2004]. The highlighted microsphere encapsulated therapeutic compounds are typically released via diffusion process, erosion process or a combination of the two processes. The PLGA backbone ester connections are hydrolyzed. This is a process; via which, erosion occurs [Zolnik & Burgess, 2007]. By adopting an oil-in-water (o/w) emulsion solvent evaporation technique, Gil-Alegre et al. produced PLGA microspheres that were loaded with BCNU for intracranial delivery. Their study showed that PLGA microspheres might release BCNU within 21 days, mostly via diffusion. They discovered through in vitro cell viability studies that the human GBM cell line (U-373 MG) included a 60% decrease rate in viability as a result of the released BCNU from PLGA microspheres, 21 days after their injection [Gil-Alegre et al., 2008]. The researchers were prompted to encapsulate TMZ into

PLGA microspheres by the fact that it included similar effectiveness as BCNU in the treatment of GBM, while including less toxicity [Adamson et al., 2009]. Low encapsulation efficiencies for the produced TMZ-loaded PLGA microspheres were reported in previous studies using o/w and water-in-oil-in-water (w/o/w) emulsion solvent evaporation methods. Poor encapsulation efficiencies discovered were caused by the fast diffusion of amphiphilic TMZ from the internal phase to the exterior water phase during the manufacturing process [Ananta et al., 2016]. Future studies should thus concentrate on enhancing encapsulation of TMZ within PLGA microspheres to decrease the quantity of medication needed for the microsphere production and increase efficiency of the procedure. The high surface energy of polymeric microspheres, which causes aggregation and complicates injection during stereotactic surgery, is the second problem associated with their use in the treatment of GBM. Last but not the least, cerebral flow causes the injected microspheres to move away from the tumor location, decreasing the efficiency of this targeted drug delivery approach [Menei et al., 1993].

Reference	Reason	Method	Results
[Li et al., 2008]	Investigation of the effect of PH on PLGA particles	solid-in-oil-in-water solvent evaporation method	Increasing pH resulted in faster drug release due to faster degradation of PLGA
[Yeo & Park, 2004]	Investigation on parameters effecting encapsulation efficiency	Emulsion solvent evaporation method was used to fabricate PLGA microspheres and characterized for encapsulation efficiency and drug release	With the increase of PLGA concentration the encapsulation efficiency also increases
[Feng et al., 2015]	Study the effect of PLGA molecular weight on the degradation and drug release behavior of PLGA microspheres	Emulsion solvent evaporation technique	With the increase of PLGA concentration the degradation rate of the particles decreases
[De & Robinson, 2004]	The effect of temperature on PLGA particles and their release profile	Particle fabricate with the use of a standard water-in-oil-in-water (w/o/w) double-emulsion	With the increase of temperature, the degradation rate increases

**Table 1.1** Overview previous work done PLGA particles

### **1.3.4 Convection-enhanced drug delivery systems**

One of the major reasons for GBM tumor recurrence includes cells that are migrating or already migrated from their original sites [Birzu et al., 2020]. Although particles and wafers are good options for the treatment, they lack specificity in this field as they cover particular areas and almost all of the migrated cells are still left untreated; thus, a method called catheter-based

convection-enhanced delivery or CED has been developed [Adamson et al., 2009]. This method provides the advantage of crossing BBB, distributing chemotherapy drugs to areas as large as the entire cerebral hemisphere and thus attacking distant invading cells [Adamson et al., 2009]. This method needs the insertion of one or more catheters powered by a motor-operated pump system with a catheter for drug delivery. It has been reported that pressure-mediated CED contributes to the homogenous distribution of therapeutic agents over a large brain area via displacing fluids [Barua et al., 2014]. Additionally, CED can deliver a wide spectrum of agents with various molecular weights and sizes [Mehta et al., 2017]. Treatment of brain tumors via the catheter-based CED method may include challenges. One of the major challenges to the use of CED in clinical settings includes backflow in the catheter [Woodworth et al., 2014]. Studies have shown that the backflow of catheters is due to several characteristics such as size, shape and how the procedure is carried out. There is always a possibility that the drug is not ultimately transferred due to leakage and wrong placement of the catheters [Woodworth et al., 2014].

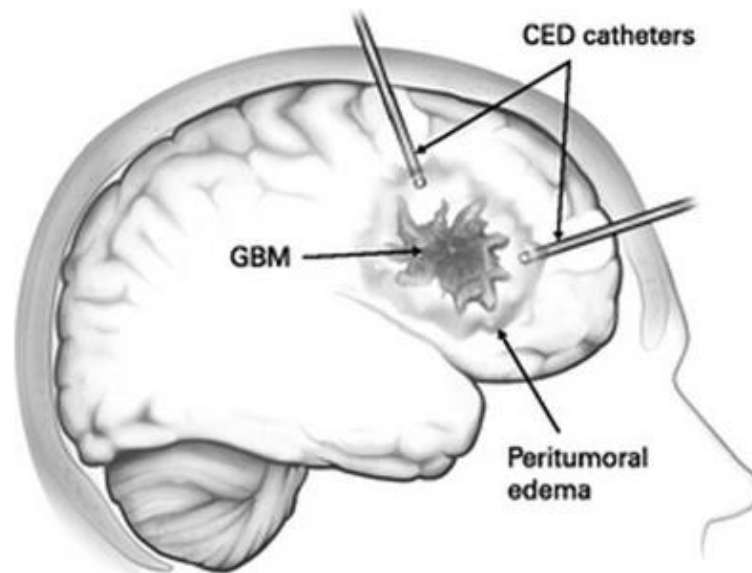


**Figure 1.6** CED use inside the anatomy of the brain; reproduced with permission [Mehta et al., 2017]

### **1.3.5 Hydrogels**

With all the available knowledge, it can confidently be addressed that the initial and integral materials used for the basis of almost all biocompatible materials are named biofibers. Biofibers are majorly segmented into four various categories of (1) natural, (2) composite, (3) synthetic and (4) hydrogel biofibers [Zwawi, 2021]. Hydrogels are among the most used biocompatible materials for cancer diagnosis and treatment [Ma et al., 2022]. Hydrogels are 3D networks of polymeric chains interconnected to each other within an aqueous environment, which is rich in water. Hydrogels are majorly insoluble due to their chemical compositions and ability to crosslink, either covalent bonds or ionic ones [Chai et al., 2017]. These characteristics of hydrogels make them different from other materials with their ability to change their structural integrity using ionic or covalent bonds. A major advantage of these hydrogels includes their ability to set into various geometries while keeping the functionality of the materials to be embedded such as cells and microparticles [El-Sherbiny & Yacoub, 2013]. However, there are numerous advantages to using hydrogels for various fields of research they do not fit in. A great disadvantage of hydrogel use is that without crosslinking agents (e.g.  $\text{CaCl}_2$  to ironically crosslink alginate), they may hardly control their geometries to meet the criteria [Bialik-Wąs et al., 2021]. Based on several studies over the past decades, hydrogels are one of the most useful materials for biocompatible drug delivery, including unique hydrogel constructions designated for tissue engineering [Fathi et al., 2015].

### **1.3.6 Mesh**

As previously stated, fiber-based fabrication plays significant roles in the development of various GBM strategies. There are five major procedures for a fiber-based scaffold fabrication (Figure 1.5): (1) electrospinning, (2) weaving, (3) knitting, (4) braiding and (5) direct writing [Tamayol et al., 2013]. Nowadays, various geometrical scaffolds are useful in tissue

engineering. These scaffolds are majorly subjected into two individual groups of (1) bulk materials such as various hydrogels and (2) fiber-based constructions. Lack of sufficient nutrients such as oxygen frequently limits high-density cell cultures. To address this need for scaffolds, direct writing methods can be created with specific geometries (especially size and pore sizes) to help nutrient absorption from desired areas [Nikolova & Chavali, 2019].

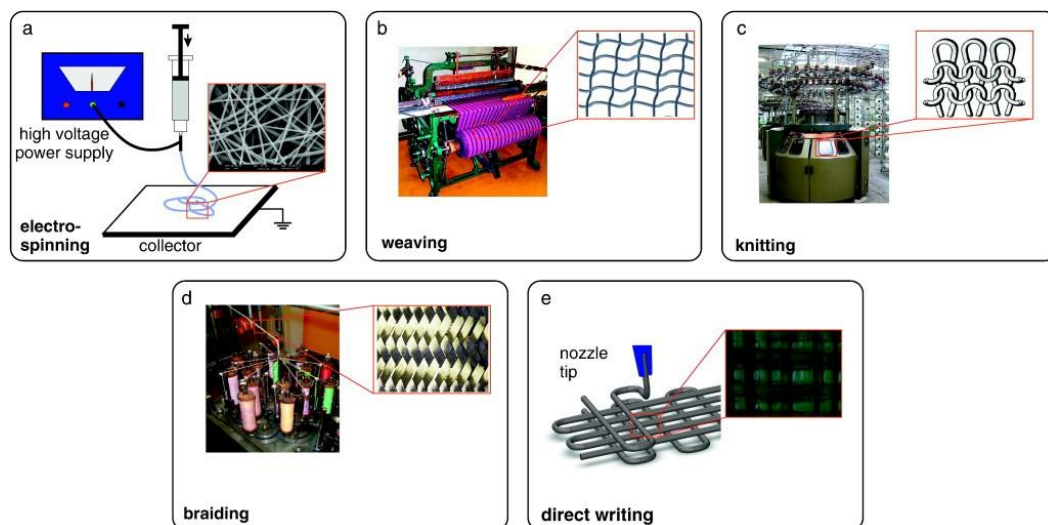


**Figure 1.7** Overview of various methods for fiber-based scaffold fabrication; reproduced with permission [Tamayol et al., 2013]

## 1.4 Conclusion

GBM is considered to be one of the most dangerous primary brain tumors in adults. Although there are available strategies of GBM treatment known as the standard of care for GBM, consisting of surgery, radiotherapy and chemo therapy, the success rate remains very low. This is due to the nature of GBM making the complete removal of the tumor extremely difficult. Furthermore, due to GBM creating hypoxic regions the efficacy of radiotherapy very low. The existence of the BBB limits the interaction of

chemotherapeutic drugs which in return develops the need for future dose resulting in health issues for example TMZ, the most widely used chemotherapeutic drug, requires high systematic doses which result in headaches, nausea and other health problems. The limitations of the above mentioned strategies for GBM brings the need for novel methods that can battle the limitations of the already available methods and to be able to carry chemotherapeutic drugs across the BBB. A great deal of potential is seen in the use of localized drug delivery systems. Each of these novel methods have their own pros and cons. Gliadel® wafers are a commercially available localized drug delivery systems that are able to deliver chemotherapeutic drugs to their designated area by bypassing the BBB. However, these wafers are large in size and rigid and require surgery to be implanted which in return could result in unseen complication and health issues. Unlike Gliadel® wafers, polymer based micro particles show promise with their ability of controlled drug release and small size to be able to be implanted with minimal surgery. Although polymeric micro particle is a great stepping point, they do have a limitation that due to the existence of the cerebral spinal fluid the particle dislodges from their original location. With this in mind researchers have gone with the use of injectable hydrogel mesh.

In this thesis we looked more into the use of embedding microparticles within an injectable hydrogel. With this research we aim to accomplish :

1. To develop biodegradable and biocompatible microparticles with the use of PLGA for the delivery chemotherapeutic drugs with hydrophilic and hydrophobic characteristics.
2. To investigate the effects of PLGA concentration on the encapsulation efficiency
3. To compare the efficiency of the different fabrication methods for the encapsulation of DFP.
4. To evaluate the morphology of the particles and the structural integrity of the microparticles.
5. To assess the release profiles of DFP-encapsulated and TMZ-encapsulated microparticles in different media (ACSF and DMEM).
6. To determine the effects of PLGA concentration on the quantity of drug

released in the media.

7. To investigate the potential use of alginate scaffolds for the delivery of DFP and TMZ.

8. To suggest potential future studies, including in vitro co-release of DFP and TMZ, cell viability assays, and in vivo studies on animal models.

For the treatment of glioblastoma (GBM), the use of a hydrogel-based mesh containing PLGA microparticles loaded with iron-chelating agents like Deferiprone (DFP) and chemotherapeutic agents like Temozolomide (TMZ) can provide a localized drug delivery system. This method may be promising for enhancing therapeutic bioavailability, lowering dosage frequency, minimizing side effects, and overcoming drug resistance. Overall, the use of PLGA microparticles, a hydrogel-based mesh, and a dual-drug delivery technique together constitutes a unique way to increase the effectiveness and lessen the side effects of treating GBM. The findings of this study shed light on the possibility of creating a tailored medication delivery system that can treat GBM while overcoming the drawbacks of systemic drug administration.

## Chapter 2

# Production of polymer-based microparticles

Oral administration of various drugs is one of the major methods of introducing specific drugs to patients [Sahoo et al., 2021]. However, this method is not an optimal choice. Oral administration of various drugs lacks the ability to target specific areas and in most cases this method increases drug courses and may lead to high toxicity levels, causing health problems [Ogu & Maxa, 2000]. Moreover, the procedure of oral administration of the drug leads to a short burst of effectiveness, which means that drugs must be readministered for good efficiency [Homayun et al., 2019]. Over the past few decades, several studies have been carried out on novel routes of drug delivery, which can control the dosage of drugs [Laffleur & Keckeis, 2020]. This method includes the use of polymer microspheres [Mitra & Dey, 2011]. The use of polymer microspheres provides a variety of advantages such as the option of various administration methods either injection or oral administration [Lengyel et al., 2019]. Furthermore, polymer microspheres can be adjusted to a point that meets the desired needs; for example, by reaching a specific site of the body drugs are introduced into the desired environment [Liechty et al., 2010]. The premise of having the ability to control doses of drugs released from these polymer microspheres goes back to the 1960s with the use of silicon rubber and polyethylene [Santini et al., 2000]. One of the major reasons for the use of polymeric microspheres includes their biocompatibility, and ability to degrade without causing health problems [Hossain et al., 2015]. Based on the current studies, it can be concluded that the use of degradable polymer microspheres is an appropriate option for controlled drug delivery at desirable body sites and drug doses without drastic invasive surgical procedures [Kamaly et al., 2016].

During the past 40 years, polyester has been a popular study subject of biocompatible structures used for drug delivery [Washington et al., 2017]. Two polyesters are included in these studies: (1) poly (lactic-co-glycolic acid) and (2) poly(lactic acid). The reason includes the fact that these polyesters are flexible and can be used for various scaffolds or drug carrier generations and have the ability to degrade without causing harm or health problems (biodegradability) [Song et al., 2018]. There are three major options for drug deliverance to the desired sites via poly(lactic-co-glycolic acid) diffusion, erosion and a combination of diffusion and erosion [Hines & Kaplan, 2013]. These highly depend on the polymer attributes. Characteristics that affect the efficacy of the delivery system are as follows: 1) copolymer ratio [Kotta et al., 2022], 2) crystallinity [Kim & Choi, 2002], 3) polymeric chains that make up the polymer, 4) preparation protocol, 5) shape and size of the microsphere particles [Yao et al., 2020], 6) drugs used for the loading of the particles, 7) porosity of the polymer and 8) environments; in which, polymer erosion occurs. The process of delivering drugs using polymeric (specifically PLGA) microsphere carriers includes three steps. First, the initial release of the drug from the microspheres can be seen. Second, a lagging phase, where doses of the drug are released and measured depending on the quantity of erosion of the microspheres. Third, secondary burst release includes almost zero order release kinetics [Silva et al, 2010; Su et al., 2021]. After being exposed to an aqueous environment, ester linkages in the PLGA microsphere are hydrolyzed, causing PLGA microsphere erosion [Zolnik & Burgess, 2007]. Lactic and glycolic acids, which are biocompatible acids, are produced as a result of this erosion [Iqbal et al., 2015]. Solubility of the therapeutic drug greatly affects which emulsion solvent evaporation process is selected over others when encapsulating therapeutic medicines into polymeric microspheres [Uchegbu & Schatzlein, 2006]. Hydrophobic medications, including hydrocortisone, prednisolone and chlorpromazine, have been encapsulated using the single o/w emulsion solvent evaporation approach [Cavalier et al., 1986]. Due to these medicinal compounds limited solubility in water, polymeric microspheres were successfully used to encapsulate the drugs [O'Donnell & McGinity, 1997]. However, due to their insolubility in the

inner oil phase, this manufacturing process is not helpful for the encapsulation of hydrophilic agents. Low encapsulation efficiency by o/w emulsion is caused due to the migration of water-soluble compounds from the oil phase to the water phase during formulation [Iqbal et al., 2015]. The w/o/w double emulsion approach is essential for encasing hydrophilic agents. This method uses an oil phase to separate the inner water phase containing the hydrophilic drug from the outer water phase. Then, polymer precipitates after the organic solvent have evaporated, which helps to achieve high encapsulation efficiencies [Alex & Bodmeier, 1990].

Previously, TMZ was encapsulated into PLGA microspheres using traditional emulsification techniques such as o/w and w/o/w. However, the encapsulation efficiency for TMZ-loaded PLGA microspheres made via the highlighted procedures has been reported low. The poor encapsulation efficiency was achieved after accounting for the partitioning of amphiphilic TMZ into the outer water phase [White et al., 2011]. Moreover, it has been suggested to saturate the external water phase with TMZ to restrict TMZ diffusion outwards and boost the encapsulation efficiency [White et al., 2011; Zhang & Gao, 2007]. These approaches are not cost-effective for the production of TMZ-loaded PLGA microspheres since a significant quantity of TMZ is consumed poorly encapsulated within the microspheres. Furthermore, high  $IC_{50}$  values of TMZ necessary for causing tumor cytotoxicity, together with the limited encapsulation of TMZ within PLGA microspheres, need excessive polymer contents for GBM cell therapy. Therefore, a significant space is available for improvements in the current design of these microspheres for the treatment of GBM [White et al., 2011].

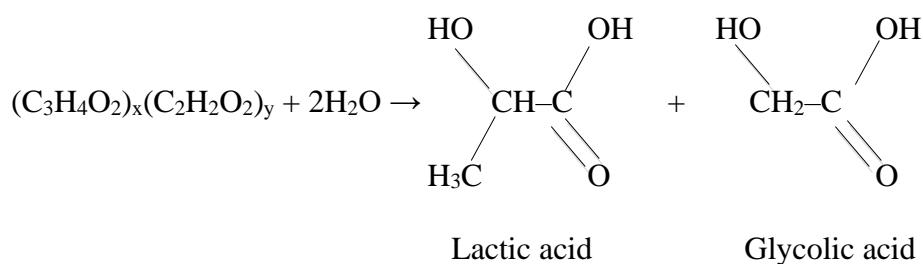


**Figure 2.1** The hydrolysis mechanism of PLGA

## **2.1 Materials and Methods**

### **2.1.1 Preparation of DFP encapsulated microparticles**

#### **Preparation of particles using w/o/w double emulsion method**

This method entailed the fabrication of PLGA particles that carry DFP [Kashi et al., 2012]. The initial step included dissolving the desired quantity of PVA in distilled water (DW) to achieve a solution of 1% PVA, which was the first aqueous phase. The solution was then mixed for 10 min at 85 °C using magnetic stirrer until PVA was fully dissolved. For the oil phase, a certain quantity of PLGA was dissolved in 3 ml of dichloromethane using vortex to completely dissolve PLGA to achieve various concentrations of 5, 10 and 15% (w/v) as the oil phase. Then, 1 ml of 1 mM DFP solution was directly added to the oil phase and vortexed for 5 min to thoroughly disperse DFP added to the solution. The first aqueous phase was mixed with the oil phase using vortex to achieve the w/o emulsion. Then, the w/o emulsion was added to 12.5 ml of 0.5% PVA solution to achieve the w/o/w emulsion. The w/o/w emulsion was added to 60 ml of 0.2% PVA. The final solution was stirred on a magnetic stirrer for 4 h at room temperature (35 °C). The solution was collected, added to conical tubes and centrifuged at 350× g for 5 min. The supernatant was collected and the allocated particles at the bottom of the tubes were washed with DW. This process was carried out three times. Moreover, particles were freeze-dried for 48 h to ensure that the particles were dried entirely, and no excess drug is left on the surface.

#### **Preparation of particles using o/o single method**

In this section, the single emulsion technique of the oil-in-oil method was used to create DFP-loaded microparticles [Mahdavi et al., 2010]. Due to the nature of DFP depicting characteristics of hydrophobic and hydrophilic attributes previously described [Su et al., 2021], a similar procedure was used to create blank microspheres. First, 3 ml of acetonitrile was transferred into a 50 ml conical tube. Then, 150, 300 and 450 mg of PLGA were added to the acetonitrile previously prepared to generate particles of 5, 10 and

15%, respectively. The resulting solution was stored, and the secondary oil phase was prepared by mixing 200  $\mu$ l of Span 80 into 40 ml of liquid paraffin. Then, half of the solution was separated and mixed with the previously prepared solution containing PLGA using vortex mixer. The solution created with the remaining solution of the secondary oil phase was combined and mixed at 55 °C for 2 h using magnetic heated stirrer to achieve blank PLGA microspheres. The resulting slush was transferred into two conical tubes and centrifuged at 350 $\times$  g for 5 min. After removal of the polymer slush supernatant, using pipettor, the remaining material was filled with DW and mixed to wash the particles using vortex. This process was repeated three times. After the final washing step, microparticles were stored for 48 h under a BSC for each organic solvent and the residue evaporated safely. The resulting particles were distributed in microtubes with each microtube including 1 mg of the particles. Microtubes were filled with 700  $\mu$ l of 1 mM DFP on top of the particles. These were stored for 72 h in the fridge to ensure that the drug was loaded in the particles efficiently. Then, the supernatant (the drug used for loading (DFP)) was removed using pipettor and a similar procedure previously described, and the particles were washed with DW and freeze-dried for 48 h to wash away extra drugs that might be left on the surface of the particles.

### **2.1.2 TMZ microparticles**

Preparation of the particles using the o/o single emulsion method was as follows: drug used for particle generation was replaced with TMZ [Rodriguez de Anda et al., 2019]. The method included a single emulsion method of using two oil phases in contrast to the previous method, which used a double emulsion method and included an aqueous phase and an oil phase. The first step was the fabrication of the first oil phase introduced. The desired quantity of PLGA powder was dissolved in 3 ml of acetonitrile and vortexed until PLGA was completely dissolved. The concentration of PLGA was assessed through the polymer over the acetonitrile (w/v%). Then, 3.75 mg of TMZ was added to the mixture to achieve the initial oil

phase. Separately, 200  $\mu$ l of Span 80 was added to 40 ml of liquid paraffin to produce the secondary oil. Then, 20 ml of the secondary oil phase was extracted and mixed with the first oil phase and the resulting solution was added to the rest of the secondary oil phase. The final solution was stirred for 2 h at 55 °C using magnetic stirrer to let the organic solvents evaporate. The resulting solution was centrifuged at 350 $\times$  g for 5 min to precipitate the fabricated microparticles. Particles were washed thrice with DW, similar to the previous method.

In fact, DFP and TMZ-loaded PLGA microspheres made from various PLGA concentrations were characterized using scanning electron microscope (SEM) (Hitachi S-4800, Japan). Briefly, 10  $\mu$ l of the produced suspensions were transferred onto SEM stubs and allowed to air dry after 1 mg of each type of the microspheres dissolved in 1 ml of anhydrous ethanol. The SEM images were captured at the desired working distances with an accelerating voltage of 1.0 kV. The SEM pictures were analyzed using commercially available ImageJ Software.

## 2.2 Results and Discussion

### 2.2.1 DFP microparticles

The fabricated DFP-loaded and encapsulated microparticles were categorized into various groups regarding their PLGA concentrations and encapsulation efficiency. Table 2.1 enlists results and categorization of the particles and effectiveness of encapsulating PLGA microspheres loaded with TMZ and DFP was assessed using the following equation:

$$\text{encapsulation efficiency (\%)} = \frac{\text{TMZ or DFP encapsulated}}{\text{TMZ or DFP theoretic}} \times 100$$

The table below shows the resulting encapsulation efficiency of various microparticles fabricated using various methods. Encapsulation efficiency of the DFP-loaded and encapsulated microparticles increased as the concentration of PLGA increased. Furthermore, the table includes various encapsulation efficiency between the two various fabrication methods with the w/o/w method of fabrication showing more promising results with increased encapsulation efficiency, compared to the o/o method of fabrication. This verified that with a specific drug of DFP that included hydrophilic and hydrophobic characteristics, the w/o/w method resulted in a better encapsulation rate. The resulting microparticles were imaged as well using S4800 Hitachi SEM (Hitachi, Japan) (Figure 2.2). The micrographs show morphology of the particles that reveal a slight difference between the particles with non-uniform size distributions between the particles. Images verify that the fabrication method and encapsulation efficiency include little effect on the structural integrity of the microparticles.

Drug encapsulated	Fabrication method	PLGA concentration	Encapsulation efficiency
DFP	o/o	5%	11.23 %
	o/o	10%	24.57 %
	o/o	15%	28.65 %
	w/o/w	5%	36.54 %
	w/o/w	10%	46.51 %
	w/o/w	15%	62.39 %
TMZ	o/o	5%	15.52 %
	o/o	10%	26.89 %
	o/o	15%	31.87 %

**Table 2.1** Overview of DFP and TMZ-loaded microparticles using various methods of fabrication based on their encapsulation efficiencies

In another study in 2015, PLGA concentration was the most crucial factor affecting characteristics of quercetin nanoparticles. Increasing PLGA concentration resulted in increases in the particle size as well as encapsulation efficiency [Tefas et al., 2015]. Thus, direct correlations were reported between the PLGA concentration and encapsulation efficiency. Both o/o and w/o/w methods have shown that when the PLGA concentration increases, encapsulation efficiency increases as well.

#### **Morphology and characterization of microparticles**

To solidify the fabrication process of the particles, whether it was TMZ encapsulated or DFP encapsulated particles, S4800 Hitachi SEM (Hitachi, Japan) was used to verify microparticle generation. Figure 2.2 shows the range and overall shape of the particles produced using o/o and w/o/w methods for TMZ and DFP, respectively. Images were recorded at 1 kV and different working distances. The quantity of PLGA used in the fabrication process included direct correlations with the size and encapsulation efficiency. With increases in PLGA, encapsulation efficiency increased as well. It is noteworthy that by increases in the concentration of

PLGA, the quantity of drugs released into the media increased.

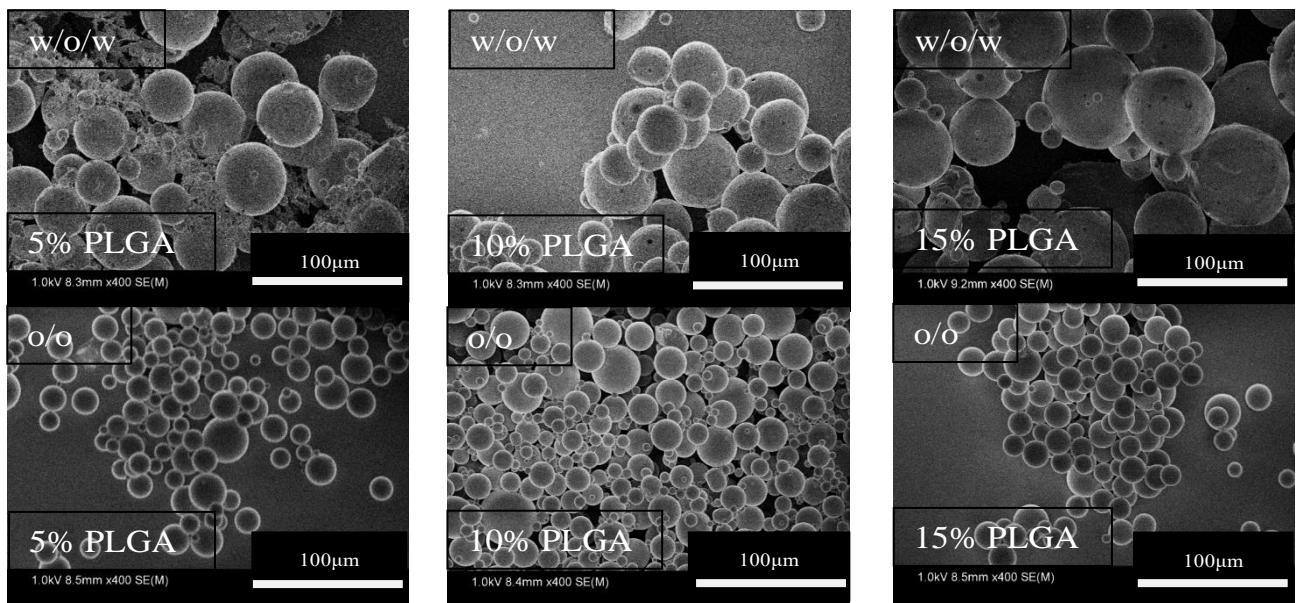


**Figure 2.2** SEM micrographs of various synthesized microparticles. First row, left to right, DFP encapsulated PLGA particles using w/o/w method at respectively 5, 10 and 15% PLGA; second row, TMZ encapsulated PLGA particles using o/o method at respectively 5, 10 and 15% PLGA

#### Cumulative release results of microparticles

Results of the release profile of DFP-loaded and encapsulated microparticles in the two media (ACSF and DMEM) for the o/o fabricated DFP-loaded microparticles demonstrated an initial release followed by a steadier and slower rate of release as time passed with the graph showing that the release almost included a plateau close to the end of the desired cycle of the experiment. In a recent study in 2020, it has been demonstrated that the size of the polymer particles strongly depends on the process variables. The most important variable for the possible changes in the process efficiency is the polymer concentration in the emulsion solution [Jajaei & Rafiei, 2020].

Figures 2.3 and 2.4 show release profiles of the o/o fabricated microparticles in ACSF and DMEM. In these figures, an initial burst release of DFP is seen, which was expected overall. By increasing the PLGA concentration, the release rate of DFP changed as the lower the PLGA concentration, the higher the overall release of DFP in media. Release of DFP in the media

occurred via diffusion and degradation rate of the PLGA microparticles. As shown in the figure, all three concentrations of PLGA microparticles included similar trends. However, with increases in PLGA concentrations, cumulative quantity of the drug released into the media changed drastically. This revealed that particles produced with 5% PLGA concentration included the maximum overall quantity of the drug released, compared to two other concentrations. Results verified the fact that by decreases in PLGA concentration, the degradation rate of the microparticles increased, resulting in further DFP loaded in the particles with a cumulative release of almost 300  $\mu\text{M}$  in ACSF. As similar release profiles between various microparticles are shown in the figure, the quantity of the released drug into the media affected the release of DFP as the overall quantity of the released drug was more than that previously assessed in ACSF. Additionally, the overall trends were similar during the first initial 24 h. After 24 h, the PLGA concentration difference affected the degradation rate of microparticles.

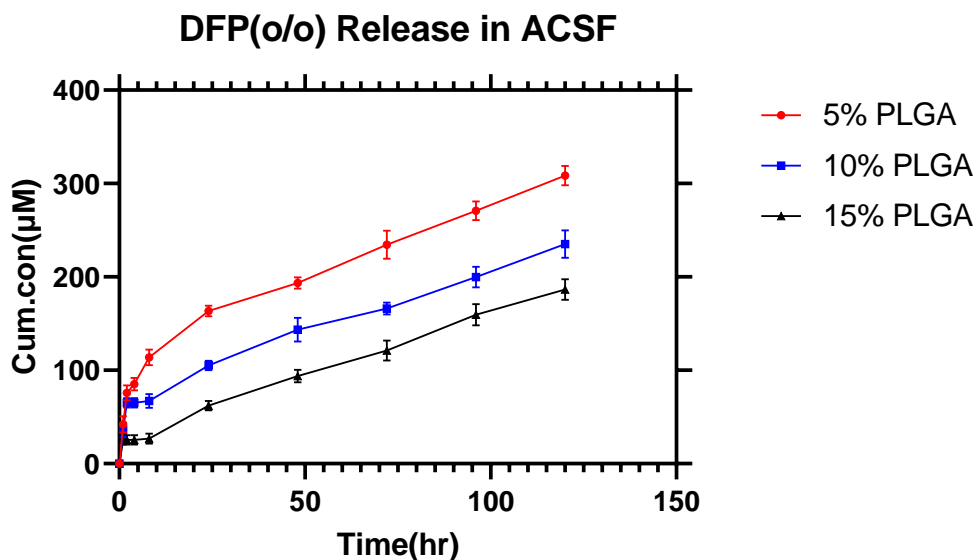


**Figure 2.3** Overview of various release profiles of DFP for various PLGA concentrations in ACSF

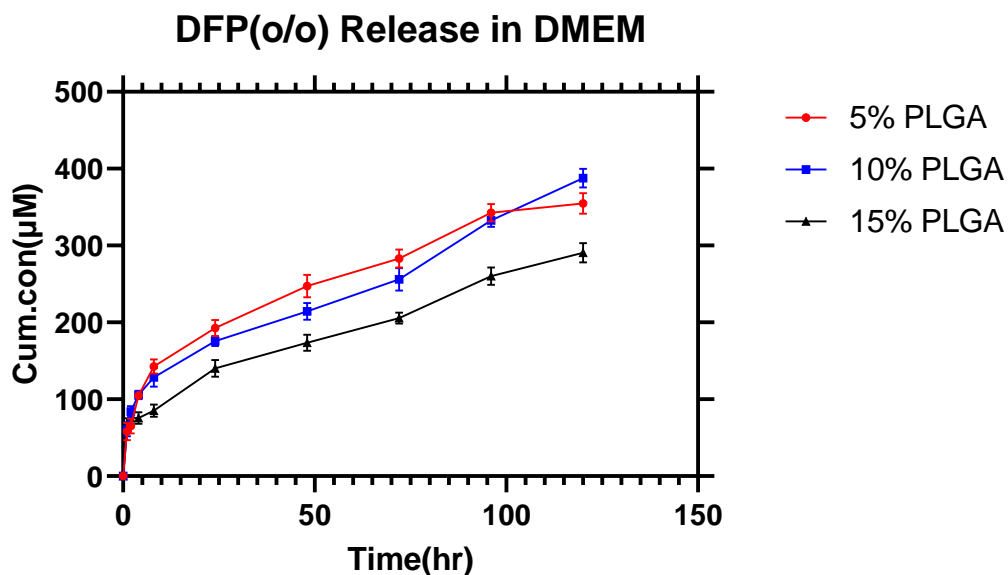


**Figure 2.4** Overview of various release profiles of DFP for various PLGA concentrations in DMEM

These results were similar to those previously recorded from releases in ACSF. We hypothesized that differences in the releases between the two media were linked to the compositions of media used in the experiment. The ACSF including components such as D-glucose, which is the most important differentiating factor between ACSF and DMEM, was used in the release of DFP. The figure also shows that release profiles of the DFP-loaded microparticles were similar between 5 and 10% PLGA concentrations. This demonstrated that the release of DFP in specific media (e.g., DMEM) did not depend highly on the concentration, except for 15% PLGA concentration with much polymer contents for the degradation effects to occur. Experiments with the use of the o/o method showed promising results. However, as stated in the previous section, encapsulation efficiency of this method was overall lower than that of the w/o/w method. This urges further experiments. Regarding the procedure for *in vitro* release of DFP using the o/o fabrication process, a similar method was used to assess the efficacy of the microparticles fabricated using w/o/w method. Figures 2.5 and 2.6 demonstrate the release rates of DFP from microparticles fabricated using the w/o/w

method. Similar results were reported; however, figures show a much faster release of DFP in the media. The overall cumulative release of DFP drastically increased, showing almost twice as much DFP released in the media with microparticles fabricated using the o/o method.

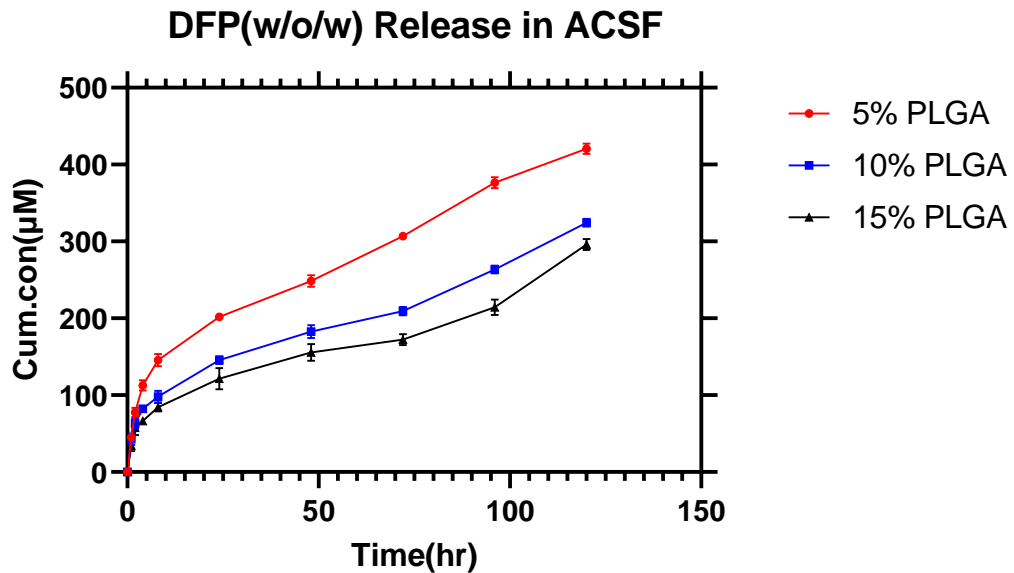


**Figure 2.5** Overview of various release profiles of DFP for various PLGA concentrations in ACSF

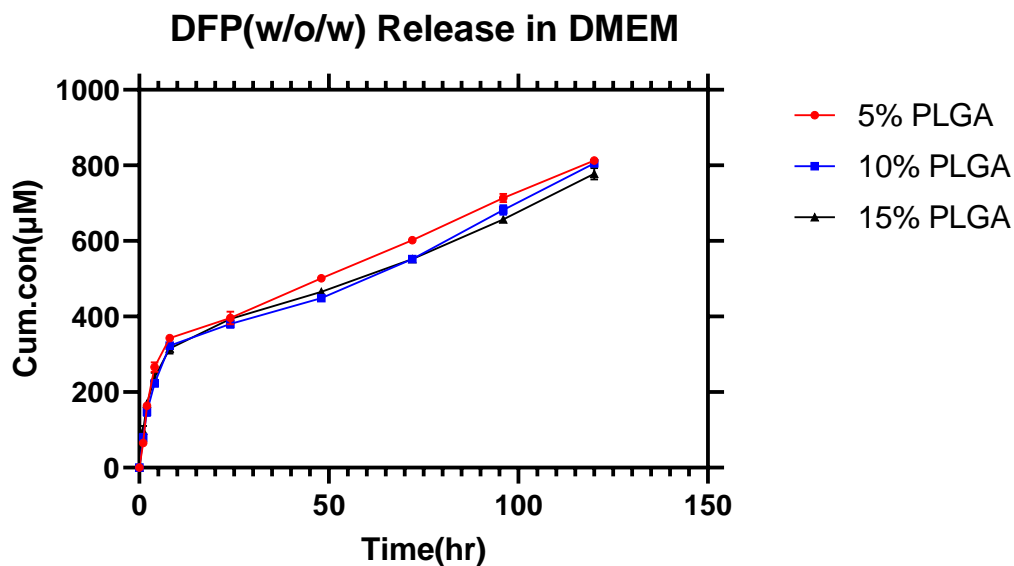


**Figure 2.6** Overview of various release profiles of DFP based on various PLGA concentrations in DMEM

Figures 2.7–2.9 characteristically show significant differences in the release profiles of DFP. Using the w/o/w method for DFP particle fabrication, encapsulation efficiency and release rate of DFP in desired environments (ACSF or DMEM) increased. The following figures further demonstrate effects of the fabrication methods used for microparticle generation. In all of the results, DFP release from the particles of various PLGA concentrations was an important factor. The resulting particles from the w/o/w fabrication method revealed a better overall release with the quantity of the cumulative DFP released almost turned to encapsulated DFP from the fabrication step. This is further verified by the encapsulation efficiency between the o/o and w/o/w processes.

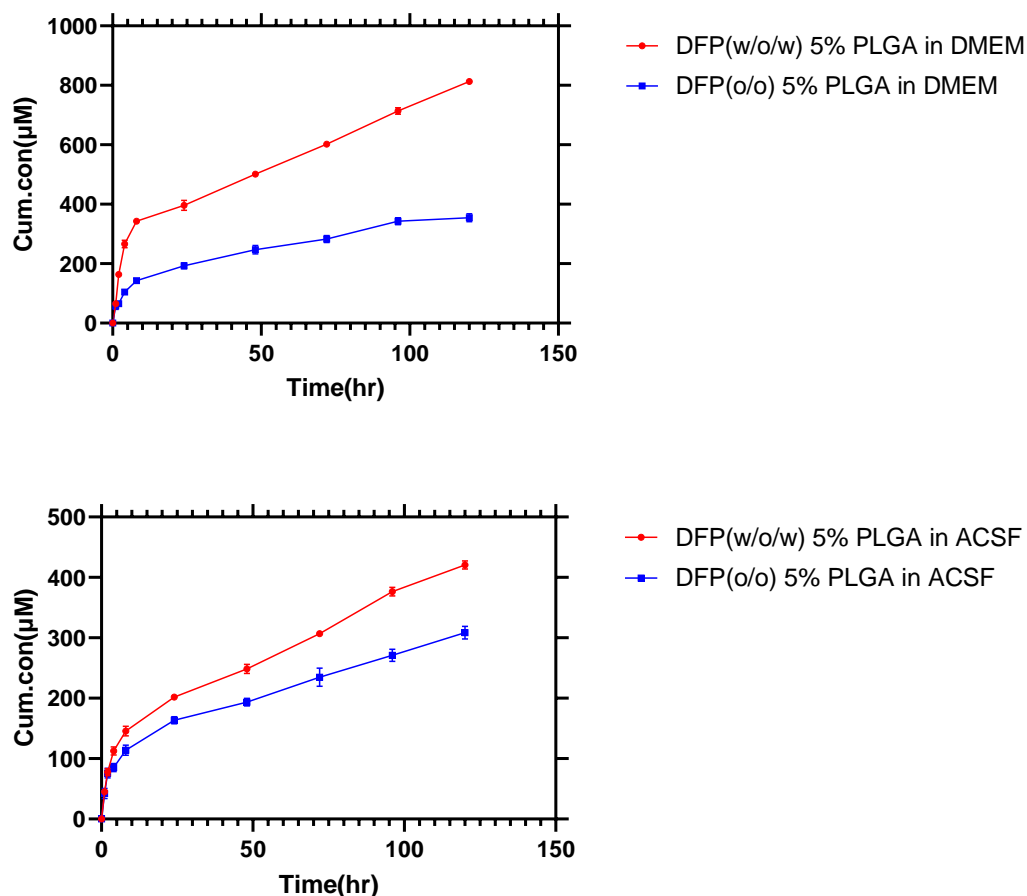


**Figure 2.7** Overview of various release profiles of DFP based on 5% PLGA concentration and fabrication methods in DMEM and ACSF

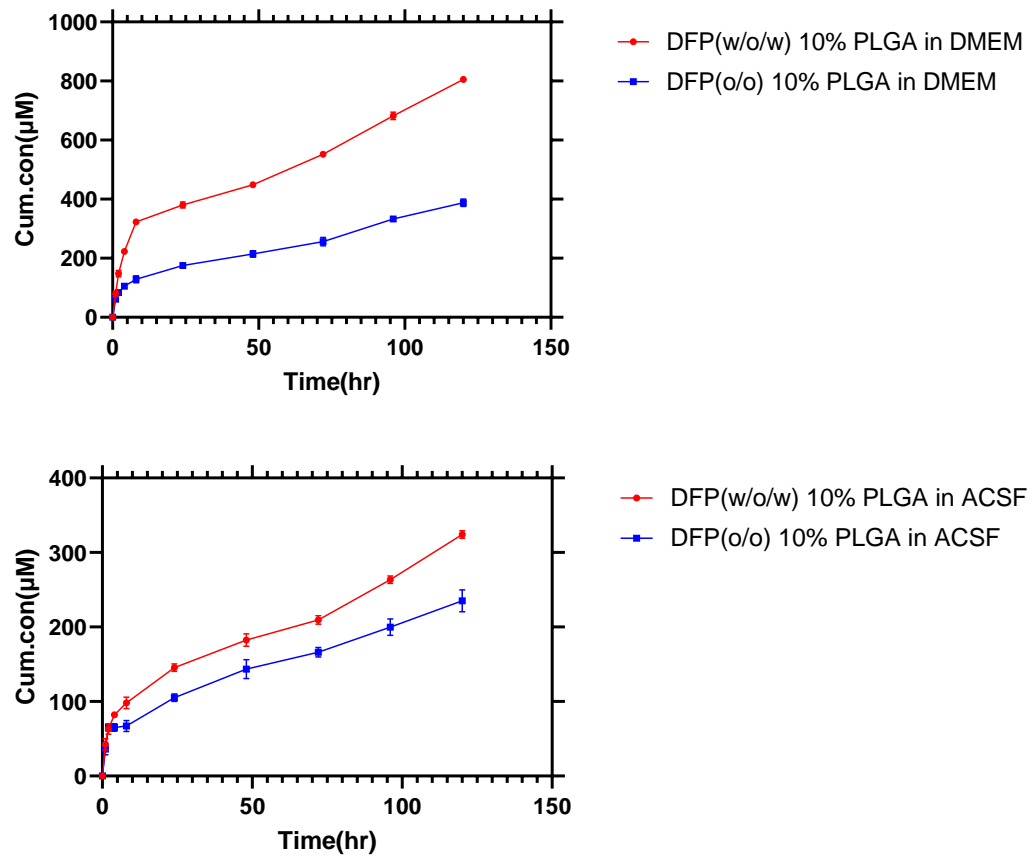


**Figure 2.8** Overview of various release profiles of DFP based on 10% PLGA concentration and fabrication methods in DMEM and ACSF

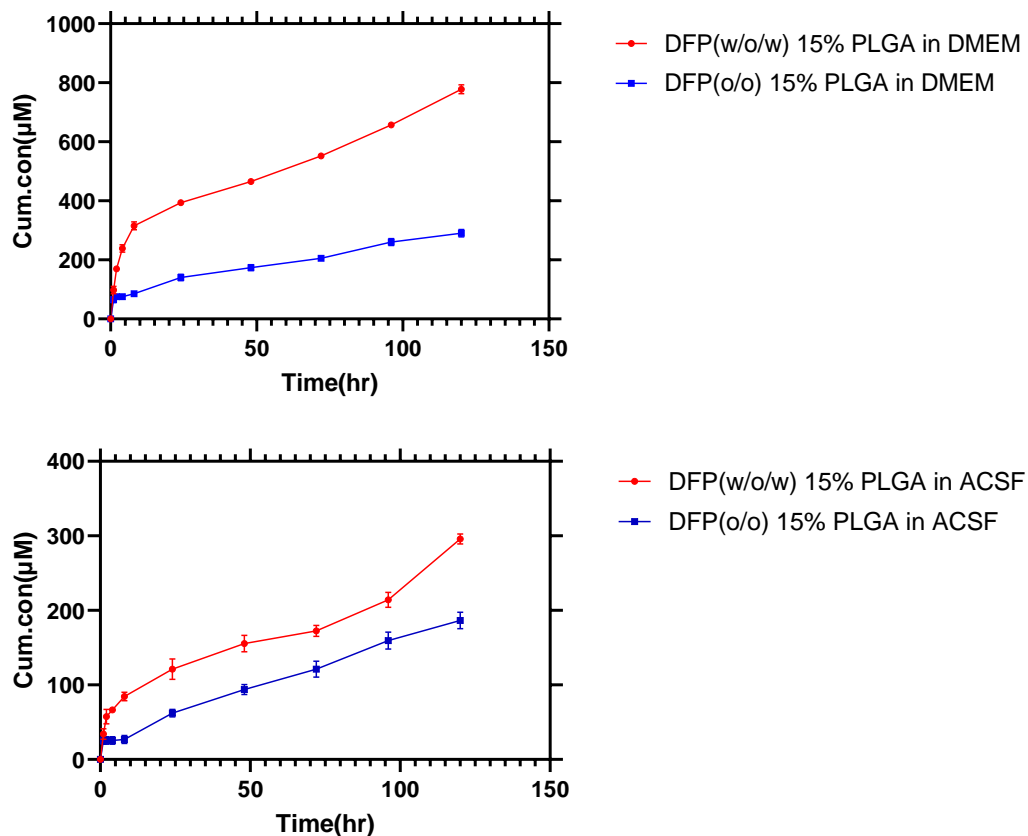


**Figure 2.9** Overview of various release profiles of DFP based on 15% PLGA concentration and fabrication methods in DMEM and ACSF

### 2.2.2 TMZ microparticles

As it is shown in Figure 2.10, TMZ release in ACSF was generally lower than its release in DMEM over 30 days. Until Day 5, drug release in all the three PLGA concentrations in ACSF was zero but since Day 5, drug release increased by 15% PLGA. However, the final release of TMZ in ACSF with 5% PLGA was the highest within other concentrations. However, TMZ release in DMEM with various PLGA concentrations included a relatively similar algorithm with the difference that the quantity of released TMZ was more than its quantity, compared to ACSF. Similar to ACSF, DMEM with 5% PLGA included the highest drug release over 30 days.

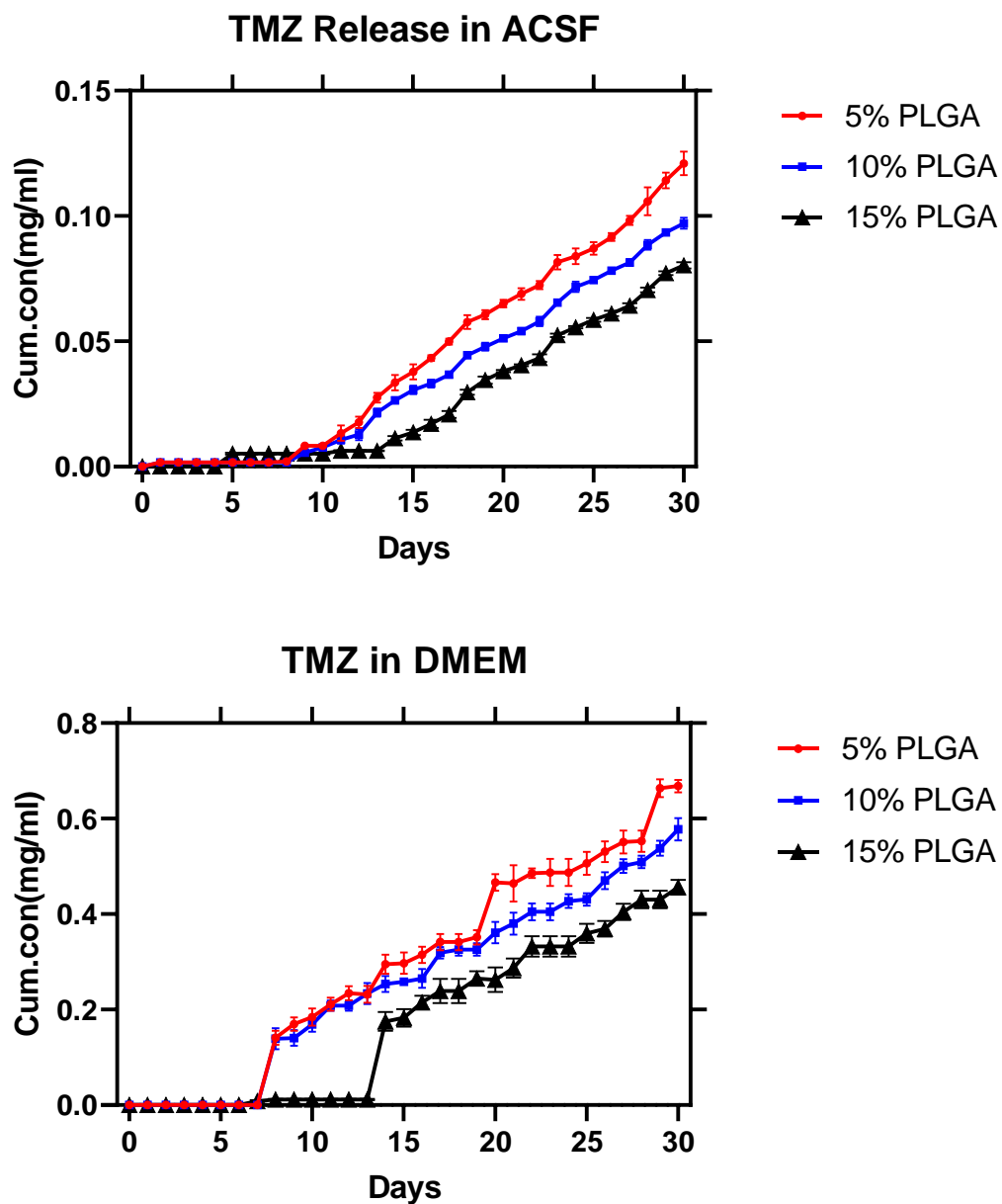


**Figure 2.10** Overview of various release profiles of TMZ based on various PLGA concentrations in ACSF and DMEM the top and bottom graph respectively

## **2.3 Conclusion**

Particles containing DFP were fabricated using two methods of o/o single emulsion and w/o/w double emulsion. Between the two fabrication methods, the w/o/w method was verified as a further efficient method of fabrication showing better encapsulation efficiency and cumulative release of DFP from the particles. Additionally, the overall release in ACSF was lower than that in DMEM. This model helped the successful production of PLGA polymer particles with DFP encapsulated for the purpose of controlled releases. This method can be further improved to better control releases of DFP. Furthermore, it has been shown that the high encapsulation efficiency using the w/o/w method had a good function by distributing the most quantity of drugs from the particles in a designated time span.

## Chapter 3

### Fabrication of alginate mesh

In biomedicine, whether it is drug delivery systems or tissue engineering, control over the quantity of drugs used for the treatment processes is becoming critical [Rambhia & Ma, 2015]. This method provides several potential advantages. Embedding microspheres can be useful to help target specific areas for treatment [Guo et al., 2014], control the dosage and quantity of drugs introduced in the system and waive needs of constant administration, which helps increase patients' compliance to the drugs. Moreover, the use of microsphere-embedded hydrogel helps prevent rapid degradation of the microspheres [Wang et al., 2021], which is a vital component that affects the efficacy and rates of the release of drugs from microparticles. This is a critical element since the goal of the design is to achieve a prolonged delivery rather than a short one. Hull was the first person to develop 3D printing in 1986 [Roopavath & Kalaskar, 2017]. The layer-by-layer material deposition is the process of 3D printing used to create 3D structures. The process first includes designing the desired mesh in a CAD (computer-aided design) model and then this is transcribed into a specific array of code (G-code) and fed into a compatible 3D printer to make the design transfer from a virtual plan to a real-life practical model. This method of mesh fabrication includes numerous advantages such as the ability to control geometry of the substrate with precision. Predominant technologies used for 3D bioprinting include (1) laser-assisted printing, (2) inkjet, and (3) microextrusion [Roopavath & Kalaskar, 2017; Murphy & Atala, 2014]. Use of extrusion-based 3D printing of hydrogels allows complex structures and geometries while still having a high resolution for printing. Furthermore, there is an option for simultaneous crosslinking or post-printing crosslinking (Figure 3.1).

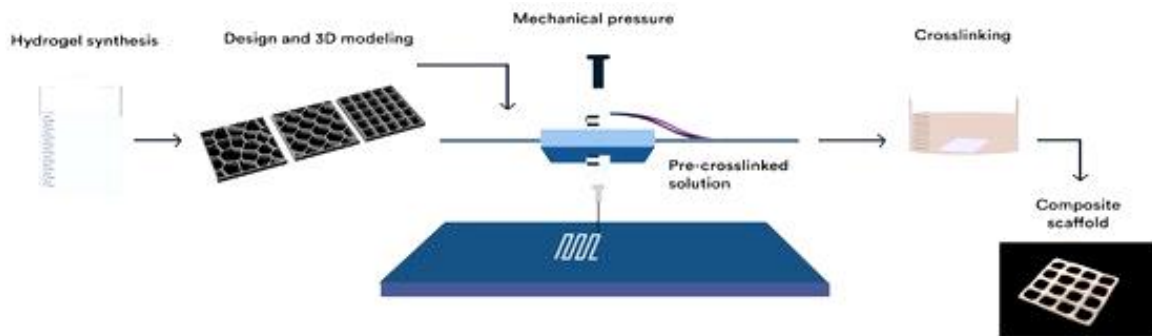


**Figure 3.1** Process of 3D printing a hydrogel from start to post fabrication crosslinking; reproduced with permission [Urruela-Barrios et al., 2019]

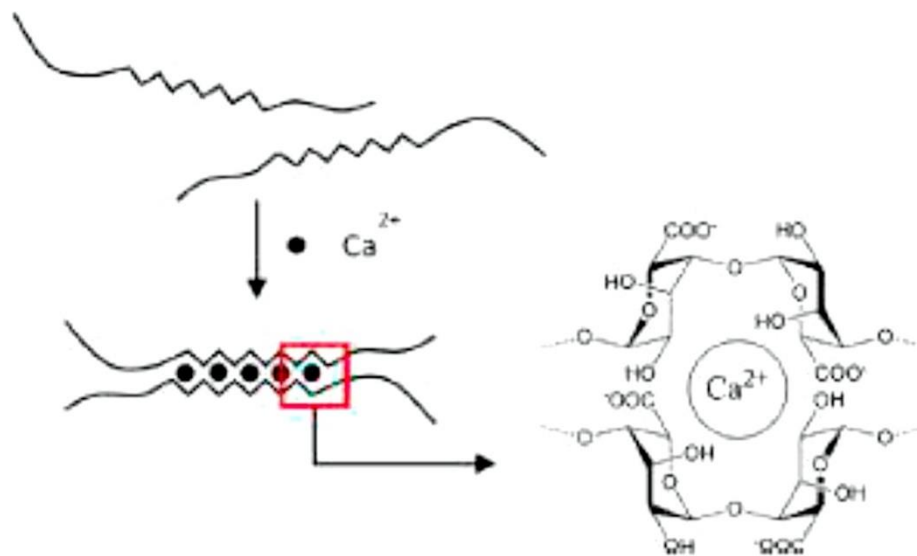


**Figure 3.2** Alginate hydrogel formation using calcium; reproduced with permission [Bonilla et al., 2018]

As previously stated, alginate is one of the most commonly used hydrogels in 3D bioprinting. Based on the nature of alginate, it can be concluded that the ability to introduce ionic crosslinking agents such as calcium (Figure 3.2) and barium makes this biochemical an appropriate option for hydrogel mesh production of various geometries. In another study, DeFail et al. designed a poly (ethylene glycol) (PEG) hydrogel loaded with microspheres for cartilage tissue engineering [DeFail et al., 2006]. As previously discussed in other chapters, the embedding of particles containing specific drugs has been verified to include several

benefits such as containing drug-eluting particles in the site and preventing them from translocation. Moreover, there is an option of further controlled releases within prolonged periods. Therefore, how extrusion-based 3D bioprinting was used for mesh fabrication was discussed in this chapter. In addition, how did the mesh affect the release of DFP encapsulated for GBM treatment was discussed as well.

## 3.1 Materials and Methods

### 3.1.1 Fabrication of the alginate scaffold

GlioMesh was created using a previously described microextrusion process by Lou et al [Luo et al., 2013]. In this method, 3D printer (CELLINK, Gothenburg, Sweden) was used to generate blank and microsphere-loaded meshes. An alginate solution with a rather high concentration (16% w/v) was printed using single-needle extrusion technique (Figure 3.3). High viscosity of this solution contributed to the structural stability of 3D bioprinted meshes.

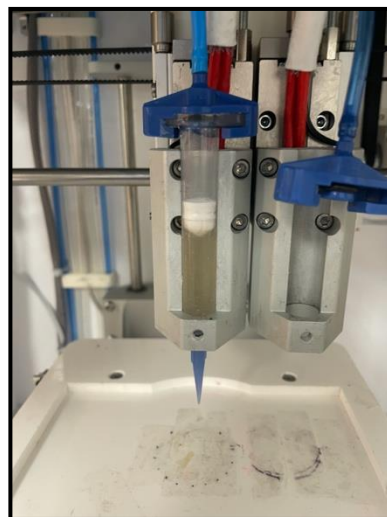


**Figure 3.3** Image of the commercial 3D bioprinter CELLINK and the single-needle extrusion technology used to prepare both blank and with microsphere-loaded meshes

Alginate powder was first weighed accurately and then dissolved in a sufficient quantity of DW to achieve an alginate solution of 16% (w/v).

The alginate solution was transferred into a CELLINK printer cartridge and installed into the 3D printer. The optimal setting for single extrusion printing of the alginate was calculated based on a study by Hosseinzadeh [Hosseinzadeh et al., 2019]. Mesh was printed at 120 kPa with a printing speed of 250 mm/min.

### **3.1.2 Fabrication of DFP microparticle loaded alginate mesh**

After the primary assessment of DFP-encapsulated microparticles, particles were distributed in a specific quantity of alginate [Pestovsky & Martínez-Antonio, 2019]. Alginate powder was added into a 3-ml syringe. The syringe tip was connected to another 3-ml syringe loaded with the desired quantity of particles using connector. The alginate and particles were then mixed by pushing the material in the two syringes very slowly to mix the particles with the alginate solution to get a homogenous distribution of particles in the alginate biofilaments. The alginate mesh was ionically crosslinked with 4%  $\text{CaCl}_2$  to improve its structural stability and maintain its form.



**Figure 3.4** Image of double-syringe method for mixing particles and alginate hydrogel

### **3.1.3**      *In vitro* release of DFP particles

After the mixing process of alginate and particles, the resulting solution was transferred to a CELLINK 3D printer. The mesh was then prepared using specific measurements of particle-to-alginate ratios, producing alginate hydrogels of 1, 3 and 6 mg/ml. Solutions were then used to prepare the alginate mesh. The alginate mesh was then transferred into Eppendorf containing ACSF and DMEM. Eppendorf was incubated at 37 °C and release rates were assessed at  $\lambda_{\text{max}} = 279$  nm using spectrophotometer. Recording of the data was carried out at specific time intervals of 1, 2, 4, 8, 24, 48, 72, 96, and 120 hr. At these time intervals, 100  $\mu\text{l}$  of the media were collected for the assessment and replaced with fresh media to ensure oversaturation of the DFP released did not occur.

In this study, cell culture media included Dulbecco's modified Eagle medium (DMEM) (Thermo Fisher Scientific, USA) supplemented with 10% of fetal bovine serum (FBS), 1% of penicillin/streptomycin (Life Technologies, USA) and 4 g/ml puromycin (Sigma-Aldrich, USA). Keeping neurons in DMEM-based culture media *in vitro* and abruptly switching to artificial cerebrospinal fluid (ACSF), the mainstay of acute electrophysiological recording for functional analysis presents a practical challenge. For short-term recording of the neuronal activity in culture and acute brain slices, a simple balanced salt solution of ACSF was prepared; however, it is not appropriate for long-term recording. Additionally, it has been demonstrated that ACSF does not include elements present in human CSF that increase neuronal excitability in slice culture [Livesey, 2015].

## 3.2 results and Discussion

After GlioMesh has been printed, the porosity afforded by the 3D structures made feasible by a 3D printer enables the flow of oxygen and nutrients to the tissue. Alginate serves as the primary bioink component in this 3D bioprinting technique, giving 3D structures a great deal of flexibility. Due to the flexible nature of GlioMesh, it is possible to make conformal contact with tissue that has an uneven shape, which helps to deliver high dosages of DFP evenly.

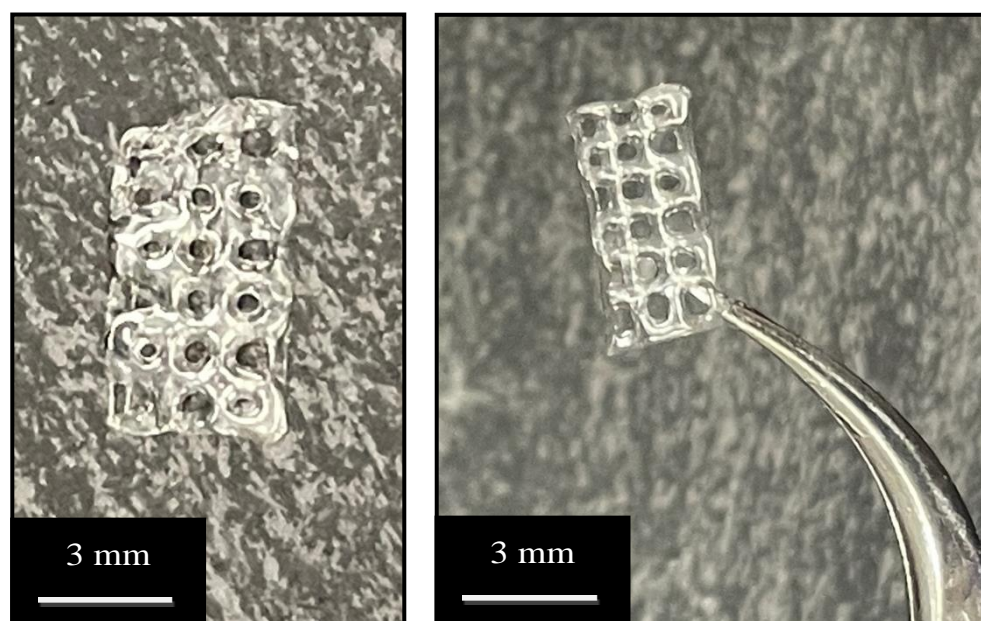


**Figure 3.5** Images of the GlioMesh post printing and crosslinking

By varying the print head pressure and printing speed, microextrusion 3D bioprinting process enables fiber diameter adjustment. The diameter of the fibers in GlioMeshes printed at various print head pressures, printing rates, and microsphere concentrations were measured. Microscopic images of alginate mesh printed with different pressures on the nozzle of 3D printer are shown in Figure below. Shown in the figure below are microscopic images of the GlioMesh with varying pressures implemented on the nozzle head from 80 kPa to 160kPa . This led to a change in porous diameter from 243  $\mu\text{m}$  to 119  $\mu\text{m}$ . We believe the cause of this is more bioink being introduced.

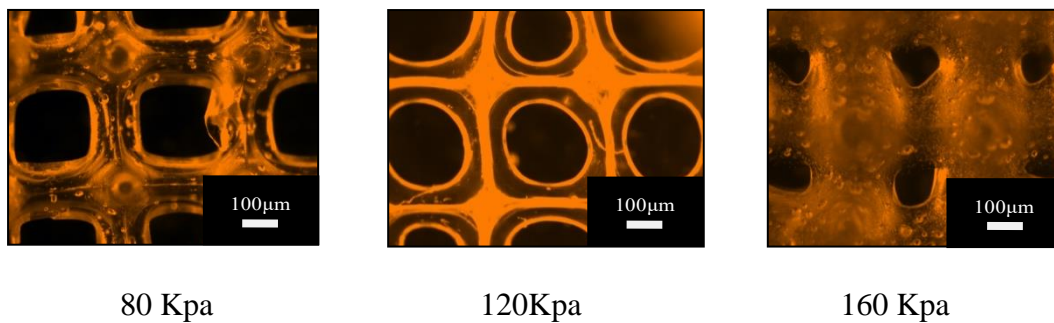


**Figure 3.6** Micrographs of alginate meshes printed using various pressures (80, 120 and 160 kPa)

Although it is demonstrated that with the increase of pressure fiber porous diameter increases the figure below demonstrates that with varying printing speed from 150 mm/min to 350 mm/min results in an increase of porous diameter from 121  $\mu\text{m}$  to 172 $\mu\text{m}$ .

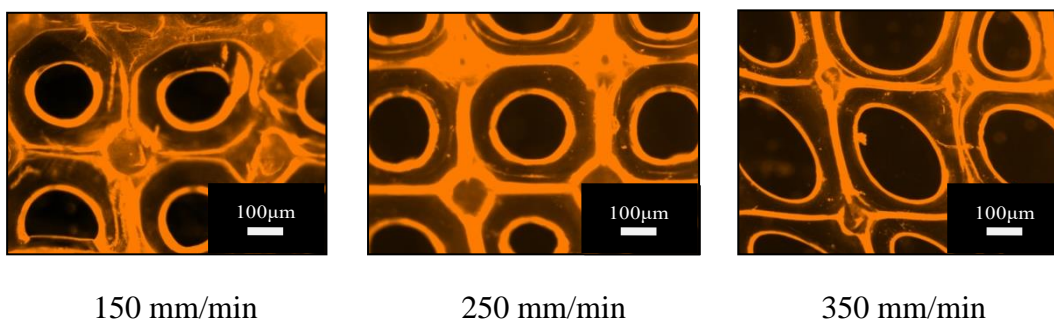


**Figure 3.7** Micrographs of alginate meshes printed using various printing speeds (150, 250 and 350 mm/min)

Additionally, it was demonstrated that the fiber porous diameter is influenced by the microsphere concentration utilized to create meshes. The density of microspheres put onto GlioMesh revealed a comparable impact on the fiber diameter as print head pressure. It was noticed that the diameter of the manufactured porous decreased from 228  $\mu\text{m}$  to 110  $\mu\text{m}$  .when the microsphere concentration was increased from 1 mg/ml to 6 mg/ml.

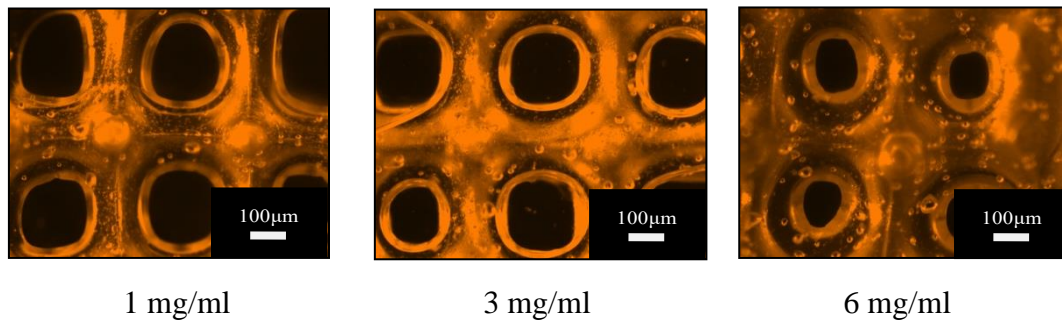
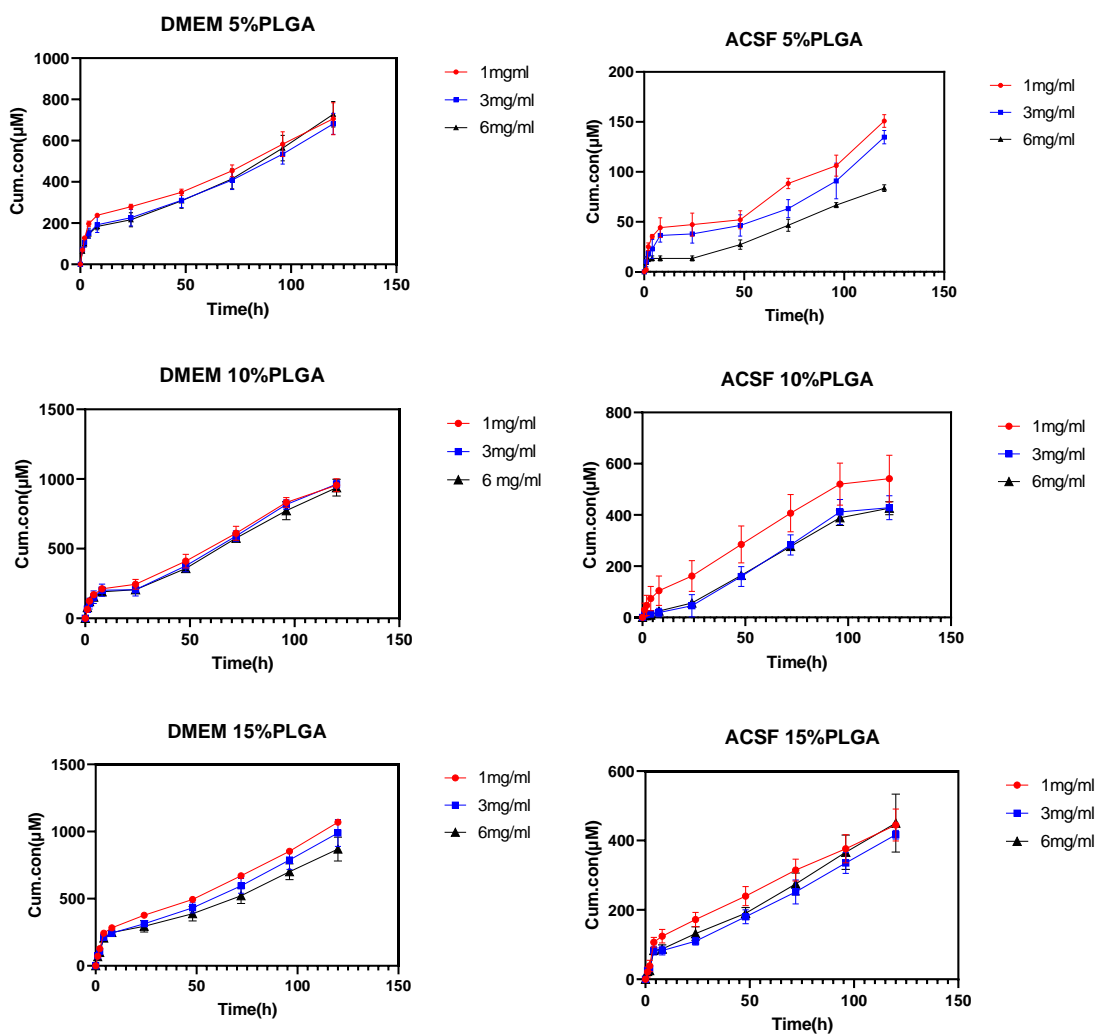


**Figure 3.8** Micrographs of alginate meshes printed using various particle concentrations (1,3 and 6 mg/ml)

In this section, the effects of DFP release from microparticles embedded in alginate fibers were discussed. Results showed differences in release profiles of the DFP-encapsulated microparticles. Significant decreases were seen in the initial release rate with a nonexistence trend in the first few periods of the measuring time (six days), as previously carried out. Release profiles of DFP particles in alginate mesh are shown in Figure 3.9. As shown in the figures, increases in the particle-to-alginate ratios included a small effect on the release rate of DFP. The hypothesis described that DFP release was delayed due to the high concentration of alginate in the experiment (16% w/v). Moreover, figures demonstrated that the rate at which DFP was released did not change dramatically. However, unlike release profiles of the particles without alginate, data included no plateau and increased with time at each measurement. As reported in previous studies that alginate slows down the release rate [Sirikia et al., 1994; Kaneko et al., 1998], this study revealed the fact that alginate use inhibited the release rate as well. As stated in previous chapters, this was more prominent in ACSF and the release rate of DFP was lower than that of DMEM. As shown in the figure, the release profile of DFP particles prepared with 10% PLGA concentration was relatively similar with a little burst with mostly a smooth profile. In this case, a burst release after 24 h. This supported the hypothesis that the DFP released from the particles stuck in the fibers and released with delay during the time points of measurement due to the porosity of

alginate. Then, it could be suggested that the release profile of DFP further depended on the quantity of DFP initially used for the particle fabrication. This behavior of similarly identical releases provides an estimation of DFP particles with a sustained release but with no countermeasures for the alginate mesh inhibitory effects on the release rate. Another reason might include the use of  $\text{CaCl}_2$  in cross-linking of the meshes as alginate can be sprayed directly into a calcium chloride solution to induce instant droplet cross-linking [Daly et al., 2020], which could provide a release environment for DFP.

**Figure 3.9** Cumulative releases of DFP encapsulated microparticles embedded in alginate meshes



### **3.3 Conclusions**

In most relative studies of recent years, 3D printing has been verified as a vital tool for the fabrication of scaffolds to help create viable efficient drug delivery systems. The use of alginate for this means includes advantages such as cost-effectiveness and biocompatibility. Moreover, the ability of the alginate hydrogels to ionically crosslink helps solidify desired shapes while maintaining their structural integrity and being flexible enough to be adapted to various environments. The geometry of a mesh is objectively important since it provides the necessary oxygen and nutrients to pass through the desired sites without delaying the release of DFP. Embedding particles in alginate scaffolds helps to keep the particles in designated sites and prevent migration of the particles. Furthermore, the distribution of the particles allows for a uniform distribution of DFP in the site. The effectiveness of the alginate with the use of embedded particles has been discussed previously. Results have shown good promises of the DFP release, which is beneficial since further controls on the release of DFP are desired.

## Chapter 4

### Conclusion and Future work

In this study, encapsulation efficiency of DFP-loaded and encapsulated particles generally increased with increasing PLGA concentration. In addition, the w/o/w method showed further promising results with improved efficiency, compared to the o/o method. This verifies that the w/o/w approach provides better encapsulation efficiency using DFP-specific drugs with hydrophilic and hydrophobic characteristics. Morphology of the particles has shown a little variation between the particles but a non-uniform size distribution between the particles. The images verify that the method and encapsulation efficiency include little effect on the structural integrity of the microparticles. The quantity of PLGA used in the process included direct correlations with the size and efficiency of the encapsulation. As PLGA increased, encapsulation efficiency increased as well. Interestingly, the quantities of drugs released in the media increased due to the increased concentration of PLGA. Results of DFP-loaded and DFP-encapsulated microparticle release profiles in the two media (ACSF and DMEM) for DFP-loaded microparticles of the o/o method showed an initial release followed by a further stable release and the slower release over time showed that the release included almost a plateau near the end of the desired cycle of the experiment.

A first burst release of DFP is usually expected. Generally, the lower the PLGA concentration that changed the DFP release rate, the higher the overall DFP release in the media. All three concentrations of PLGA microparticles showed similar results. However, as the concentration of PLGA increased, cumulative quantity of drug released in the media changed dramatically. This showed that the particles produced with 5% PLGA concentration included the maximum total quantity of the released drug, compared to the other two concentrations. Decreasing the concentration of PLGA increased the rate of microparticle degradation, which resulted in

loading of further DFP into the particles, with a cumulative release rate in ACSF. Since similar release profiles between various microparticles were shown, the quantity of drug released in the media affected the release of DFP as the total quantity of released drug was greater than that previously assessed in ACSF. In fact, encapsulation efficiency of this method was generally lower than that of the w/o/w method. In the current study, the total cumulative release of DFP increased dramatically, releasing nearly twice as much DFP into the microparticle media produced using the o/o method. In all the results, DFP release from particles of various PLGA concentrations was an important factor. The resulting particles from the w/o/w fabrication method revealed a better overall release with the cumulatively released quantity of DFP almost changed to encapsulated DFP from the fabrication step.

Recently, 3D printing has become an important tool for the fabrication of scaffolds to help researchers develop efficient and viable drug delivery systems. Advantages of such use of alginate include cost-effectiveness and biocompatibility. In addition, the ability of the alginate hydrogels to form ionic cross-links helps them harden their desired shapes while maintaining their structural integrity. This is also flexible enough to adapt to various environments. Furthermore, the geometry of meshes is essential as it provides oxygen and nutrients needed to pass through the desired sites without slowing the release of DFP. The inclusion of particles in the alginate scaffolds helps the scaffolds keep the particles in designated places as well as prevent migration of the particles. Additionally, particle distribution ensures even distributions of DFP across the sites. In conclusion, results of the present study have suggested that good DFP release schemes are overall beneficial; however, further controls of the DFP release are necessary.

Future studies can include *in vivo* co-release of DFP and TMZ as well as cell viability assay according to specific IC<sub>50</sub> values. This thesis has shown great potential in a hydrogel-based particle-embedded mesh for the delivery of iron-chelating agents. One thing that is observed through the results is a correlation between the particle size and drug concentration on the final

release. The data suggests that with the increase in particle size, the amount of anticancer drug that can be encapsulated also increases, which in return causes a higher cumulative concentration. This can be studied further to understand the relation better and to generate more efficient microparticles. The next step would be to consider *in vivo* studies to determine how efficiently can the co-release of the drugs be improved upon. Another potential outlook would be to consider a study based on how toxic or safe this could be. Before the hydrogel mesh can be used in human clinical trials, the safety and toxicity of the mesh must be assessed.

Furthermore, the developed Alginate mesh can also be investigated on animal models as a potential *in vitro* extension of this study. Because combining various antitumor drugs with TMZ and DFP inhibits tumor development synergistically, this characteristic can be added to alginate meshes and its usefulness assessed. By adding pH-responsive characteristics to alginate meshes, differences in pH between tumors and healthy tissues may be leveraged to make drug delivery systems smarter. These studies will help better understand the needed quantity of anticancer drugs and the time needed for administration.

Overall, this project's future work in the areas of *in vivo* drug release and *in vitro* animal studies may contribute to the creation of a safe and efficient drug administration method for treating glioblastoma.

# Appendix A

## Additional Information

### Fabrication of PLGA microparticles with three methods:

#### 1. Water/Oil/Water

a. The first aqueous phase ( $W_1$ ) was prepared by dissolving a certain concentration of PVA to achieve a 1% w/v PVA solution.

b. This was then emulsified with 3 mL of a dichloromethane (DCM) solution containing the desired concentration of PLGA (vortexing for one minute).

Note: PLGA should be dissolved initially in 3ml DCM.

c. The primary W/O emulsion was dispersed into 20 mL of 0.5% w/v PVA solution ( $W_1$ ) and vortex for one minute.

d. The W/O/W emulsion was added to 80 mL of 0.2% w/v PVA solution and stirred at 35 °C for 4 h to allow the organic solvent to evaporate.

e. The final suspension was centrifuged to collect the microspheres, which were washed thrice with distilled water and then freeze-dried.

#### 2. Water/Oil/Oil

a. The first aqueous phase ( $W_1$ ) was prepared by dissolving a certain concentration of PVA to achieve 1% w/v PVA solution.

b.  $W_1$  was then emulsified with 5 mL of acetonitrile (ACN) solution containing of the desired concentration of PLGA (vortexing for one minute).

c. 100 mL of viscous liquid paraffin containing 5% of Span 80 was used as the second oil phase ( $O_2$ ).

d. The W/O emulsion was then emulsified by the 20 ml of second oil phase using a vortex mixer.

f. The W/O/O was added to 80 mL of  $O_2$  and stirred at 35 °C for 4 h to allow the organic solvent to evaporate.

e. The microspheres were collected by centrifugation and washed thrice with *n*-hexane and lyophilized.

### 3. Oil/Oil

- a) Prepare the first oil phase (O1): weight and put in the amount of PLGA for desired final concentration.
- b) Add 3 ml of in the tube and vortex until PLGA is completely dissolved.
- c) Weight 3.75 mg of TMZ and add it to the dissolved PLGA.
- d) Prepare the second oil phase (O2): 40 mL of viscous liquid then add 200  $\mu$ L of Span 80.
- e) Add O1, all volume, into the tube and as fast as possible, close the tube and vortex for 1 minute.
- f) let it stir for 2 hours at 55 °C.
- g) put the solution into a 50 ml tube and centrifuge at 250 xg for 5 minutes.
- h) Remove the supernatant as much as possible and add 40 ml of n-Hexane. Centrifuge again.
- i) Repeat this operation other 2 times.
- j) Let the particles dry for 24-48 h under the chemical hood or in the tube or in a glass petri dish.

### 4. *In vitro* Drug Release

- a. Suspending 1 mg microspheres in 700  $\mu$ l of the desired media under research
- b. Samples were vortex and placed in the incubator and maintained at 37 °C.
- c. At predefined time intervals, the samples were taken out of the incubator, vortexed and centrifuged at 12000 rpm for 5 min.
- d. Medium was completely withdrawn for analysis and fresh medium of equal volume was added in the meantime.
- e. The precipitated microsphere pellets were resuspended in the medium and placed back in the incubator.
- f. The drug concentration in the supernatant was determined fluorometrically (TMZ: 327 nm, DFP: 279 nm).
- g. The cumulative release was determined.

# Bibliography

[Abbruzzese et al., 2022] Abbruzzese, C., Persico, M., Matteoni, S., & Paggi, M. G. (2022). Molecular Biology in Glioblastoma Multiforme Treatment. *Cells*, 11(11), 1850.

[Adamson et al., 2009] Adamson, C., Kanu, O. O., Mehta, A. I., Di, C., Lin, N., Mattox, A. K., and Bigner, D. D. (2009). Glioblastoma multiforme: a review of where we have been and where we are going. *Expert Opinion on Investigational Drugs*, 18(8):1061–1083.

[Aldoghachi et al., 2022] Aldoghachi, A. F., Aldoghachi, A. F., Bryne, K., Ling, K. H., & Cheah, P. S. (2022). Recent advances in the therapeutic strategies of glioblastoma multiforme. *Neuroscience*.

[Alex & Bodmeier, 1990] Alex, R., & Bodmeier, R. (1990). Encapsulation of water-soluble drugs by a modified solvent evaporation method. I. Effect of process and formulation variables on drug entrapment. *Journal of microencapsulation*, 7(3), 347-355.

[Ananta et al., 2016] Ananta, J. S., Paulmurugan, R., and Massoud, T. F. (2016). Temozolomide-loaded plga nanoparticles to treat glioblastoma cells: a biophysical and cell culture evaluation. *Neurological Research*, 38(1):51–59. PMID: 26905383.

[Asija et al., 2022] Asija, S., Chatterjee, A., Yadav, S., Chekuri, G., Karulkar, A., Jaiswal, A. K., Goda, J. S., and Purwar, R. (2022). Combinatorial approaches to effective therapy in glioblastoma (gbm): Current status and what the future holds. *International Reviews of Immunology*, 0(0):1–24. PMID: 35938932.

[Auffinger et al., 2015] Auffinger, B., Spencer, D., Pytel, P., Ahmed, A. U., & Lesniak, M. S. (2015). The role of glioma stem cells in chemotherapy resistance and glioblastoma multiforme recurrence. *Expert Review of Neurotherapeutics*, 15(7), 741–752.

[Bao et al., 2021] Bao, C., Zhang, J., Xian, S. Y., & Chen, F. (2021). MicroRNA-670-3p suppresses ferroptosis of human glioblastoma cells through targeting ACSL4. *Free Radical Research*, 55(7), 743-754.

[Barua et al., 2014] Barua, N. U., Gill, S. S., & Love, S. (2014). Convection-enhanced drug delivery to the brain: Therapeutic potential and neuropathological considerations. *Brain Pathology*, 24(2), 117–127.

[Bausart et al., 2022] Bausart, M., Pr eat, V., and Malfanti, A. (2022). Immunotherapy for glioblastoma: the promise of combination strategies. *Journal of Experimental & Clinical Cancer Research*, 41(1):1–22.

[Bialik-Wa et al., 2021] Bialik-Wa, K., Krolicka, E., & Malina, D. (2021). Impact of the type of crosslinking agents on the properties of modified sodium alginate/poly (Vinyl alcohol) hydrogels. *Molecules*, 26(8), 2381.

[Birzu et al., 2020] Birzu, C., French, P., Caccese, M., Cerretti, G., Idbah, A., Zagonel, V., & Lombardi, G. (2020). Recurrent glioblastoma: from molecular landscape to new treatment perspectives. *Cancers*, 13(1), 47.

[Candolfi et al., 2014] Candolfi, M., Yagiz, K., Wibowo, M., Ahlzadeh, G. E., Puntel, M., Ghiasi, H., ... & Castro, M. G. (2014). Temozolomide Does Not Impair Gene Therapy-Mediated Antitumor Immunity in Syngeneic Brain Tumor Models. Temozolomide Combined with Immunotherapy for the Treatment of Glioblastoma Multiforme. *Clinical Cancer Research*, 20(6), 1555–1565.

[Cavalier et al., 1986] Cavalier, M., Benoit, J. P., & Thies, C. (1986). The formation and characterization of hydrocortisone-loaded poly ((±)-lactide) microspheres. *Journal of pharmacy and pharmacology*, 38(4), 249-253.

[Chai et al., 2017] Chai, Q., Jiao, Y., & Yu, X. (2017). Hydrogels for biomedical applications: their characteristics and the mechanisms behind them. *Gels*, 3(1), 6.

[Chao et al., 2001] Chao, K. C., Bosch, W. R., Mutic, S., Lewis, J. S., Dehdashti, F., Mintun, M. A., Dempsey, J. F., Perez, C. A., Purdy, J. A., and Welch, M. J. (2001). A novel approach to overcome hypoxic tumor resistance: Cu-atom-guided intensity-modulated radiation therapy. *International Journal of Radiation Oncology\* Biology\* Physics*, 49(4):1171–1182.

[Chowdhury et al., 2021] Chowdhury, S., Bappy, M. H., Clocchiatti-Tuozzo, S., Cheeti, S., Chowdhury, S., & Patel, V. (2021). Current Advances in Immunotherapy for Glioblastoma Multiforme and Future Prospects. *Cureus*, 13(12).

[Citrin & Mitchell, 2014] Citrin, D. E., & Mitchell, J. B. (2014). Altering the response to radiation: sensitizers and protectors. *In Seminars in Oncology* (Vol. 41, No. 6, pp. 848–859). WB Saunders.

[Combs et al., 2008] Combs, S. E., Wagner, J., Bischof, M., Welzel, T., Wagner, F., Debus, J., and Schulz-Ertner, D. (2008). Postoperative treatment of primary glioblastoma multiforme with radiation and concomitant temozolomide in elderly patients. *International Journal of Radiation Oncology\* Biology\* Physics*, 70(4):987–992.

[Daly et al., 2020] Daly, A. C., Riley, L., Segura, T., & Burdick, J. A. (2020). Hydrogel microparticles for biomedical applications. *Nature Reviews Materials*, 5(1), 20–43.

[De, S., & Robinson, D. H., 2004] Particle size and temperature effect on the physical stability of PLGA nanospheres and microspheres containing Bodipy. *AAPS PharmSciTech*, 5(4), 53-53.

[DeFail et al., 2006] DeFail, A. J., Chu, C. R., Izzo, N., & Marra, K. G. (2006). Controlled release of bioactive TGF- $\beta$ 1 from microspheres embedded within biodegradable hydrogels. *Biomaterials*, 27(8), 1579–1585.

[Diaz-Cano, 2012] Diaz-Cano, S. J. (2012). Tumor heterogeneity: mechanisms and bases for a reliable application of molecular marker design. *International Journal of Molecular Sciences*, 13(2), 1951–2011.

[Dixon et al., 2012] Dixon, S. J., Lemberg, K. M., Lamprecht, M. R., Skouta, R., Zaitsev, E. M., Gleason, C. E., ... & Stockwell, B. R. (2012). Ferroptosis: an iron-dependent form of nonapoptotic cell death. *Cell*, 149(5), 1060-1072.

[El-Khayat & Arafat, 2021] El-Khayat, S. M., & Arafat, W. O. (2021). Therapeutic strategies of recurrent glioblastoma and its molecular pathways ‘Lock up the beast’. *ecancermedicalscience*, 15.

[El-Sherbiny & Yacoub, 2013] El-Sherbiny, I. M., & Yacoub, M. H. (2013). Hydrogel scaffolds for tissue engineering: Progress and challenges. *Global Cardiology Science and Practice*, 2013(3), 38.

[Entezari et al., 2022] Entezari, S., Haghi, S. M., Norouzkhani, N., Sahebazar, B., Vosoughian, F., Akbarzadeh, D., ... & Deravi, N. (2022). Iron Chelators in Treatment of Iron Overload. *Journal of Toxicology*, 2022.

[Fabro et al., 2022] Fabro, F., Lamfers, M. L., & Leenstra, S. (2022). Advancements, challenges, and future directions in tackling glioblastoma resistance to small kinase inhibitors. *Cancers*, 14(3), 600.

[Fan et al., 2013] Fan, C. H., Liu, W. L., Cao, H., Wen, C., Chen, L., & Jiang, G. (2013). O6-methylguanine DNA methyltransferase as a promising target for the treatment of temozolomide-resistant gliomas. *Cell Death & Disease*, 4(10), e876–e876.

[Fathi et al., 2015] Fathi, M., Barar, J., Aghanejad, A., & Omid, Y. (2015). Hydrogels for ocular drug delivery and tissue engineering. *BioImpacts: BI*, 5(4), 159.

[Feng, S., Nie, L., Zou, P., & Suo, J., 2015] Effects of drug and polymer molecular weight on drug release from PLGA-mPEG microspheres. *Journal of Applied Polymer Science*, 132(6).

[Fernandes et al., 2017] Fernandes, C., Costa, A., Osorio, L., Lago, R. C., Linhares, P., Carvalho, B., & Caeiro, C. (2017). Current standards of care in glioblastoma therapy. *Exon Publications*, 197–241.

[Flynn et al., 2008] Flynn, J. R., Wang, L., Gillespie, D. L., Stoddard, G. J., Reid, J. K., Owens, J., Ellsworth, G. B., Salzman, K. L., Kinney, A. Y., and Jensen, R. L. (2008). Hypoxia-regulated protein expression, patient characteristics, and preoperative imaging as predictors of survival in adults with glioblastoma multiforme. *Cancer*, 113(5):1032–1042.

[Funes et al., 2019] Funes, S. C., de Lara, A. M., Altamirano-Lagos, M. J., Mackern-Oberti, J. P., Escobar-Vera, J., & Kalergis, A. M. (2019). Immune checkpoints and the regulation of tolerogenicity in dendritic cells: implications for autoimmunity and immunotherapy. *Autoimmunity Reviews*, 18(4), 359–368.

[Germano et al., 2010] Germano, I., Swiss, V., & Casaccia, P. (2010). Primary brain tumors, neural stem cell, and brain tumor cancer cells: where is the link?. *Neuropharmacology*, 58(6), 903–910.

[Gil-Alegre et al., 2008] Gil-Alegre, M., Gonzalez-Alvarez, I., Gutierrez-Pauls, L., and Torres-Suárez, A. I. (2008). Three weeks release BCNU loaded hydrophilic-plga microspheres for interstitial chemotherapy: Development and activity against human glioblastoma cells. *Journal of Microencapsulation*, 25(8):561–568.

[Grochans et al., 2022] Grochans, S., Cybulska, A. M., Simińska, D., Korbecki, J., Kojder, K., Chlubek, D., & Baranowska-Bosiacka, I. (2022). Epidemiology of Glioblastoma Multiforme—Literature Review. *Cancers*, 14(10), 2412.

[Guerin et al., 2004] Guerin, C., Olivi, A., Weingart, J. D., Lawson, H. C., and Brem, H. (2004). Recent advances in brain tumor therapy: local intracerebral drug delivery by polymers. *Investigational New Drugs*, 22(1):27–37.

- [Guo et al., 2014] Guo, X., Zhang, X., Ye, L., Zhang, Y., Ding, R., Hao, Y., ... & Zhang, Y. (2014). Inhalable microspheres embedding chitosan-coated PLGA nanoparticles for 2-methoxyestradiol. *Journal of Drug Targeting*, 22(5), 421-427.
- [Hanif et al., 2017] Hanif, F., Muzaffar, K., Perveen, K., Malhi, S. M., & Simjee, S. U. (2017). Glioblastoma multiforme: a review of its epidemiology and pathogenesis through clinical presentation and treatment. *Asian Pacific Journal of Cancer Prevention: APJCP*, 18(1), 3.
- [Heath et al., 2013] Heath, J. L., Weiss, J. M., Lavau, C. P., & Wechsler, D. S. (2013). Iron deprivation in cancer—potential therapeutic implications. *Nutrients*, 5(8), 2836–2859.
- [Hentze et al., 2010] Hentze, M. W., Muckenthaler, M. U., Galy, B., & Camaschella, C. (2010). Two to tango: regulation of Mammalian iron metabolism. *Cell*, 142(1), 24-38.
- [Hines & Kaplan, 2013] Hines, D. J., & Kaplan, D. L. (2013). Poly(lactic-co-glycolic)acid– controlled-release systems: experimental and modeling insights. *Critical Reviews in Therapeutic Drug Carrier Systems*, 30(3).
- [Homayun et al., 2019] Homayun, B., Lin, X., & Choi, H. J. (2019). Challenges and recent progress in oral drug delivery systems for biopharmaceuticals. *Pharmaceutics*, 11(3), 129.
- [Hossain et al., 2015] Hossain, K. M. Z., Patel, U., & Ahmed, I. (2015). Development of microspheres for biomedical applications: a review. *Progress in Biomaterials*, 4(1), 1–19.
- [Hosseinzadeh et al., 2019] Hosseinzadeh, R., Mirani, B., Pagan, E., Mirzaaghaei, S., Nasimian, A., Kawalec, P., ... & Akbari, M. (2019). A drug-eluting 3D-printed mesh (GlioMesh) for management of glioblastoma. *Advanced Therapeutics*, 2(11), 1900113.
- [Hou et al., 2006] Hou, L. C., Veeravagu, A., Hsu, A. R., and Tse, V. C. K. (2006). Recurrent glioblastoma multiforme: a review of natural history and management options. *Neurosurgical Focus FOC*, 20(4):E3.

- [Iqbal et al., 2015] Iqbal, M., Zafar, N., Fessi, H., & Elaissari, A. (2015). Double emulsion solvent evaporation techniques used for drug encapsulation. *International journal of pharmaceutics*, 496(2), 173-190.
- [Jadhav et al., 2007] Jadhav, V., Solaroglu, I., Obenaus, A., & Zhang, J. H. (2007). Neuroprotection against surgically induced brain injury. *Surgical Neurology*, 67(1), 15–20.
- [Jajaei & Rafiei, 2020] Jajaei, M. S., & Rafiei, S. (2020). Preparation of drug delivery system based on poly (lactide-glycolide) and evaluation of parameters affecting its structure for cancer treatment. *South African Journal of Chemical Engineering*, 33, 107–115.
- [Jawhari et al., 2016] Jawhari, S., Ratinaud, M.-H., and Verdier, M. (2016). Glioblastoma, hypoxia and autophagy: a survival-prone ‘menage-a-trois’. *Cell death & Disease*, 7(10):e2434–e2434.
- [Jovcevska, 2019] Jovcevska, I. (2019). Genetic secrets of long-term glioblastoma survivors. *Bosnian Journal of Basic Medical Sciences*, 19(2), 116.
- [Kamaly et al., 2016] Kamaly, N., Yameen, B., Wu, J., & Farokhzad, O. C. (2016). Degradable controlled-release polymers and polymeric nanoparticles: mechanisms of controlling drug release. *Chemical Reviews*, 116(4), 2602–2663.
- [Kanderi & Gupta, 2021] Kanderi, T., & Gupta, V. (2021). Glioblastoma multiforme. In StatPearls [Internet]. *StatPearls Publishing*.
- [Kaneko et al., 1998] Kaneko, K., Kanada, K., Miyagi, M., Saito, N., Ozeki, T., Yuasa, H., & Kanaya, Y. (1998). Formation of water-insoluble gel in dry-coated tablets for the controlled release of theophylline. *Chemical and Pharmaceutical Bulletin*, 46(4), 728–729.
- [Kashi et al., 2012] Kashi, T. S. J., Eskandarion, S., Esfandyari-Manesh, M., Marashi, S. M. A., Samadi, N., Fatemi, S. M., ... & Dinarvand, R. (2012). Improved drug loading and antibacterial activity of minocycline-loaded PLGA nanoparticles prepared by solid/oil/water ion pairing method. *International Journal of Nanomedicine*, 7, 221.

[Kim & Choi, 2002] Kim, J. H., & Choi, H. K. (2002). Effect of additives on the crystallization and the permeation of ketoprofen from adhesive matrix. *International Journal of Pharmaceutics*, 236(1-2), 81-85.

[Klingenschmid et al., 2022] Klingenschmid, J., Krigers, A., Kerschbaumer, J., Thomé, C., Pinggera, D., & Freyschlag, C. F. (2022). Surgical Management of Malignant Glioma in the Elderly. *Frontiers in Oncology*, 12.

[Korolnek & Hamza, 2015] Korolnek, T., & Hamza, I. (2015). Macrophages and iron trafficking at the birth and death of red cells. *Blood, The Journal of the American Society of Hematology*, 125(19), 2893–2897.

[Kotta et al., 2022] Kotta, S., Aldawsari, H. M., Badr-Eldin, S. M., Nair, A. B., & Yt, K. (2022). Progress in Polymeric Micelles for Drug Delivery Applications. *Pharmaceutics*, 14(8), 1636.

[Krishnareddy & Swaminath, 2014] Krishnareddy, S., & Swaminath, A. (2014). When combination therapy isn't working: emerging therapies for the management of inflammatory bowel disease. *World Journal of Gastroenterology: WJG*, 20(5), 1139.

[Laffleur & Keckeis, 2020] Laffleur, F., & Keckeis, V. (2020). Advances in drug delivery systems: Work in progress still needed?. *International Journal of Pharmaceutics*, 590, 119912.

[Lane et al., 2014] Lane, D. J., Mills, T. M., Shafie, N. H., Merlot, A. M., Moussa, R. S., Kalinowski, D. S., ... & Richardson, D. R. (2014). Expanding horizons in iron chelation and the treatment of cancer: Role of iron in the regulation of ER stress and the epithelial–mesenchymal transition. *Biochimica et Biophysica Acta (BBA)-Reviews on Cancer*, 1845(2), 166-181.

[Lara-Velazquez et al., 2021] Lara-Velazquez, M., Shireman, J. M., Lehrer, E. J., Bowman, K. M., Ruiz-Garcia, H., Paukner, M. J., ... & Dey, M. (2021). A comparison between chemo-radiotherapy combined with immunotherapy and chemo-radiotherapy alone for the treatment of newly diagnosed glioblastoma: a systematic review and meta-analysis. *Frontiers in oncology*, 11, 662302.

[Lengyel et al., 2019] Lengyel, M., Kállai-Szabó, N., Antal, V., Laki, A. J., & Antal, I. (2019). Microparticles, microspheres, and microcapsules for advanced drug delivery. *Scientia Pharmaceutica*, 87(3), 20.

[Li et al., 2018] Li, X., Shao, C., Shi, Y., & Han, W. (2018). Lessons learned from the blockade of immune checkpoints in cancer immunotherapy. *Journal of Hematology & Oncology*, 11(1), 1–26.

[Liechty et al., 2010] Liechty, W. B., Kryscio, D. R., Slaughter, B. V., & Peppas, N. A. (2010). Polymers for drug delivery systems. *Annual Review of Chemical and Biomolecular Engineering*, 1, 149.

[Li, J., Jiang, G., & Ding, F., 2008] The effect of pH on the polymer degradation and drug release from PLGA-mPEG microparticles. *Journal of Applied Polymer Science*, 109(1), 475-482.

[Livesey, 2015] Livesey, F. J. (2015). Reconstructing the neuronal milieu interieur. *Proceedings of the National Academy of Sciences*, 112(20), 6250–6251.

[Luo et al., 2013] Luo, Y., Lode, A., & Gelinsky, M. (2013). Direct Plotting of Three-Dimensional Hollow Fiber Scaffolds Based on Concentrated Alginate Pastes for Tissue Engineering. *Advanced Healthcare Materials*, 2(6), 777–783. <https://doi.org/10.1002/adhm.201200303>

[Ma et al., 2022] Ma, J., Wang, B., Shao, H., Zhang, S., Chen, X., Li, F., & Liang, W. (2022). Hydrogels for localized chemotherapy of liver cancer: a possible strategy for improved and safe liver cancer treatment. *Drug Delivery*, 29(1), 1457–1476.

[Mahdavi et al., 2010] Mahdavi, H., Mirzadeh, H., Hamishehkar, H., Jamshidi, A., Fakhari, A., Emami, J., ... & Nokhodchi, A. (2010). The effect of process parameters on the size and morphology of poly (d, l-lactide-co-glycolide) micro/nanoparticles prepared by an oil in oil emulsion/solvent evaporation technique. *Journal of Applied Polymer Science*, 116(1), 528–534.

- [Makadia & Siegel, 2011] Makadia, H. K., & Siegel, S. J. (2011). Poly lactic-co-glycolic acid (PLGA) as biodegradable controlled drug delivery carrier. *Polymers*, 3(3), 1377–1397.
- [Mehta et al., 2017] Mehta, A. M., Sonabend, A. M., & Bruce, J. N. (2017). Convection-enhanced delivery. *Neurotherapeutics*, 14(2), 358–371.
- [Menei et al., 1993] Menei, P., Daniel, V., Montero-Menei, C., Brouillard, M., Pouplard-Barthelaix, A., and Benoit, J. (1993). Biodegradation and brain tissue reaction to poly (d, l-lactide-co-glycolide) microspheres. *Biomaterials*, 14(6):470–478.
- [Mesfin & Al-Dhahir, 2017] Mesfin, F. B., & Al-Dhahir, M. A. (2017). Gliomas. In *StatPearls* [Internet]. StatPearls Publishing. Last accessed 23 October, 2022.
- [Mitra & Dey, 2011] Mitra, A., & Dey, B. (2011). Chitosan microspheres in novel drug delivery systems. *Indian Journal of Pharmaceutical Sciences*, 73(4), 355.
- [Mobarra et al., 2016] Mobarra, N., Shanaki, M., Ehteram, H., Nasiri, H., Sahmani, M., Saeidi, M., ... & Azad, M. (2016). A review on iron chelators in treatment of iron overload syndromes. *International Journal of Hematology-Oncology and Stem Cell Research*, 10(4), 239.
- [Mokhtari et al., 2017] Mokhtari, R. B., Homayouni, T. S., Baluch, N., Morgatskaya, E., Kumar, S., Das, B., & Yeger, H. (2017). Combination therapy in combating cancer. *Oncotarget*, 8(23), 38022.
- [Murphy & Atala, 2014] Murphy, S. V., & Atala, A. (2014). 3D bioprinting of tissues and organs. *Nature Biotechnology*, 32(8), 773–785.
- [Nazemi-Gelyan, 2015] Nazemi-Gelyan, H., Hasanzadeh, H., Makhdumi, Y., Abdollahi, S., Akbari, F., Varshoe-Tabrizi, F., ... & Rezaei-Tavirani, M. (2015). Evaluation of organs at risk's dose in external radiotherapy of brain tumors. *Iranian journal of cancer prevention*, 8(1), 47.

- [Nikolova & Chavali, 2019] Nikolova, M. P., & Chavali, M. S. (2019). Recent advances in biomaterials for 3D scaffolds: A review. *Bioactive Materials*, 4, 271–292.
- [O'Donnell & McGinity, 1997] O'Donnell, P. B., & McGinity, J. W. (1997). Preparation of microspheres by the solvent evaporation technique. *Advanced drug delivery reviews*, 28(1), 25-42.
- [Ogu & Maxa, 2000] Ogu, C. C., & Maxa, J. L. (2000). Drug interactions due to cytochrome P450. In *Baylor University Medical Center Proceedings* (Vol. 13, No. 4, pp. 421–423). Taylor & Francis.
- [Ohgaki and Kleihues, 2012] Ohgaki, H. and Kleihues, P. (2012). The definition of primary and secondary glioblastoma. *Clinical Cancer Research*, 19:764 – 772.
- [Omuro and DeAngelis, 2013] Omuro, A. and DeAngelis, L. M. (2013). Glioblastoma and Other Malignant Gliomas: A Clinical Review. *JAMA*, 310(17):1842–1850.
- [Parisi et al., 2015] Parisi, S., Corsa, P., Raguso, A., Perrone, A., Cossa, S., Munafò, T., ... & Valle, G. (2015). Temozolomide and radiotherapy versus radiotherapy alone in high grade gliomas: a very long term comparative study and literature review. *BioMed Research International*, 2015.
- [Pearson et al., 2020] Pearson, J. R., Cuzzubbo, S., McArthur, S., Durrant, L. G., Adhikaree, J., Tinsley, C. J., ... & McArdle, S. E. (2020). Immune escape in glioblastoma multiforme and the adaptation of immunotherapies for treatment. *Frontiers in Immunology*, 11, 582106.
- [Pestovsky & Martínez-Antonio, 2019] Pestovsky, Y. S., & Martínez-Antonio, A. (2019). The Synthesis of Alginate Microparticles and Nanoparticles. *Drug Des Intellect Prop Int J*, 3(1), 293–327.
- [Pinto & Forni, 2020] Pinto, V. M., & Forni, G. L. (2020). Management of iron overload in beta-thalassemia patients: clinical practice update based on case series. *International Journal of Molecular Sciences*, 21(22), 8771.

[Poon et al., 2020] Poon, M. T., Sudlow, C. L., Figueroa, J. D., & Brennan, P. M. (2020). Longer-term ( $\geq 2$  years) survival in patients with glioblastoma in population-based studies pre-and post-2005: a systematic review and meta-analysis. *Scientific Reports*, 10(1), 1–10.

[Rambhia & Ma, 2015] Rambhia, K. J., & Ma, P. X. (2015). Controlled drug release for tissue engineering. *Journal of Controlled Release*, 219, 119-128.

[Rasel & Mahboobi, 2022] Rasel, M., & Mahboobi, S. K. (2022). Transfusion Iron Overload. In *StatPearls* [Internet]. StatPearls Publishing. Last accessed 23 October, 2022.

[Rodriguez de Anda et al., 2019] Rodriguez de Anda, D. A., Ohannesian, N., Martirosyan, K. S., & Chew, S. A. (2019). Effects of solvent used for fabrication on drug loading and release kinetics of electrosprayed temozolomide-loaded PLGA microparticles for the treatment of glioblastoma. *Journal of Biomedical Materials Research Part B: Applied Biomaterials*, 107(7), 2317–2324.

[Roopavath & Kalaskar, 2017] Roopavath, U. K., & Kalaskar, D. M. (2017). Introduction to 3D printing in medicine. In *3D printing in medicine* (pp. 1-20). Woodhead Publishing.

[Rouault, 2006] Rouault, T. A. (2006). The role of iron regulatory proteins in mammalian iron homeostasis and disease. *Nature Chemical Biology*, 2(8), 406-414.

[S Hersh, 2016] S Hersh, D., S Wadajkar, A., B Roberts, N., G Perez, J., P Connolly, N., Frenkel, V., ... & J Kim, A. (2016). Evolving drug delivery strategies to overcome the blood brain barrier. *Current Pharmaceutical Design*, 22(9), 1177–1193.

[Sahoo et al., 2021] Sahoo, Deviprasad, et al. "Oral drug delivery of nanomedicine." *Theory and Applications of Nonparenteral Nanomedicines*. Academic Press, 2021. 181–207.

[Santini et al., 2000] Santini, Jr, John T., et al. "Microchips as controlled drug-delivery devices." *Angewandte Chemie International Edition* 39.14 (2000): 2396–2407.

- [Sarkar & Kellogg, 2010] Sarkar, A., & Kellogg, G. E. (2010). Hydrophobicity-shake flasks, protein folding and drug discovery. *Current Topics in Medicinal Chemistry*, 10(1), 67–83.
- [Schonberg et al., 2015] Schonberg, D. L., Miller, T. E., Wu, Q., Flavahan, W. A., Das, N. K., Hale, J. S., ... & Rich, J. N. (2015). Preferential iron trafficking characterizes glioblastoma stem-like cells. *Cancer Cell*, 28(4), 441-455.
- [Sharpe, 2009] Sharpe, A. H. (2009). Mechanisms of costimulation. *Immunological Reviews*, 229(1), 5.
- [Silva et al, 2010] Silva, A. R. D., Zaniquelli, M. E. D., Baratti, M. O., & Jorge, R. A. (2010). Drug release from microspheres and nanospheres of poly (lactide-co-glycolide) without sphere separation from the release medium. *Journal of the Brazilian Chemical Society*, 21, 214-225.
- [Sirkiä et al., 1994] Sirkiä, T., Salonen, H., Veski, P., Jürjenson, H., & Marvola, M. (1994). Biopharmaceutical evaluation of new prolonged-release press-coated ibuprofen tablets containing sodium alginate to adjust drug release. *International Journal of Pharmaceutics*, 107(3), 179–187.
- [Song et al., 2018] Song, R., Murphy, M., Li, C., Ting, K., Soo, C., & Zheng, Z. (2018). Current development of biodegradable polymeric materials for biomedical applications. *Drug Design, Development and Therapy*, 12, 3117.
- [Sparrow, 2010] Sparrow, R. L. (2010). Red blood cell storage and transfusion-related immunomodulation. *Blood Transfusion*, 8(Suppl 3), s26.
- [Stewart and Burdett, 2002] Stewart, L. and Burdett, S. (2002). Chemotherapy for high-grade glioma. *Cochrane Database of Systematic Reviews*, (4).
- [Strobel et al., 2019] Strobel, H., Baisch, T., Fitzel, R., Schilberg, K., Siegelin, M. D., Karpel-Massler, G., ... & Westhoff, M. A. (2019). Temozolomide and other alkylating agents in glioblastoma therapy. *Biomedicines*, 7(3), 69.

[Stupp et al., 2005] Stupp, R., Mason, W. P., Van Den Bent, M. J., Weller, M., Fisher, B. (2005). Radiotherapy plus concomitant and adjuvant temozolomide for glioblastoma. *N Engl J Med*, 352(10), 987–96.

[Su et al., 2021] Su, Y., Zhang, B., Sun, R., Liu, W., Zhu, Q., Zhang, X., ... & Chen, C. (2021). PLGA-based biodegradable microspheres in drug delivery: recent advances in research and application. *Drug Delivery*, 28(1), 1397–1418.

[Tamayol et al., 2013] Tamayol, A., Akbari, M., Annabi, N., Paul, A., Khademhosseini, A., & Juncker, D. (2013). Fiber-based tissue engineering: Progress, challenges, and opportunities. *Biotechnology Advances*, 31(5), 669–687.

[Tefas et al., 2015] Tefas, L. R., Tomuta, I., Achim, M., & Vlase, L. (2015). Development and optimization of quercetin-loaded PLGA nanoparticles by experimental design. *Clujul Med*, 88(2), 214–223. doi:10.15386/cjmed-418

[Thakkar et al., 2014] Thakkar, J. P., Dolecek, T. A., Horbinski, C., Ostrom, Q. T., Lightner, D. D., Barnholtz-Sloan, J. S., and Villano, J. L. (2014). Epidemiologic and molecular prognostic review of glioblastomagbm epidemiology and biomarkers. *Cancer Epidemiology, Biomarkers & Prevention*, 23(10):1985–1996.

[Turnquist, Harris, & Harris, 2020] Turnquist, C., Harris, B. T., & Harris, C. C. (2020). Radiation-induced brain injury: current concepts and therapeutic strategies targeting neuroinflammation. *Neuro-Oncology Advances*, 2(1), vdaa057.

[Uchegbu & Schatzlein, 2006] Uchegbu, I. F., & Schatzlein, A. G. (Eds.). (2006). *Polymers in drug delivery*. CRC Press.

[Valdes et al., 2010] Valdes, P. A., Samkoe, K., O'Hara, J. A., Roberts, D. W., Paulsen, K. D., & Pogue, B. W. (2010). Deferoxamine iron chelation increases  $\delta$ -aminolevulinic acid induced protoporphyrin IX in xenograft glioma model. *Photochemistry and Photobiology*, 86(2), 471–475.

[Vanneman & Dranoff, 2012] Vanneman, M., & Dranoff, G. (2012). Combining immunotherapy and targeted therapies in cancer treatment. *Nature Reviews Cancer*, 12(4), 237–251.

[Viswanathan et al., 2017] Viswanathan, V. S., Ryan, M. J., Dhruv, H. D., Gill, S., Eichhoff, O. M., Seashore-Ludlow, B., ... & Schreiber, S. L. (2017). Dependency of a therapy-resistant state of cancer cells on a lipid peroxidase pathway. *Nature*, 547(7664), 453-457.

[Vo et al., 2022] Vo, V. T., Kim, S., Hua, T. N., Oh, J., & Jeong, Y. (2022). Iron commensalism of mesenchymal glioblastoma promotes ferroptosis susceptibility upon dopamine treatment. *Communications Biology*, 5(1), 1-14.

[Wang et al., 2017] Wang, Z., Yang, G., Zhang, Y. Y., Yao, Y., & Dong, L. H. (2017). A comparison between oral chemotherapy combined with radiotherapy and radiotherapy for newly diagnosed glioblastoma: a systematic review and meta-analysis. *Medicine*, 96(44).

[Wang et al., 2021] Wang, S., Shi, K., Lu, J., Sun, W., Han, Q., Che, L., & Zhang, D. (2021). Microsphere-Embedded Hydrogel Sustained-Release System to Inhibit Postoperative Epidural Fibrosis. *ACS Applied Bio Materials*, 4(6), 5122-5131.

[Washington et al., 2017] Washington, K. E., Kularatne, R. N., Karmegam, V., Biewer, M. C., & Stefan, M. C. (2017). Recent advances in aliphatic polyesters for drug delivery applications. *Wiley Interdisciplinary Reviews: Nanomedicine and Nanobiotechnology*, 9(4), e1446.

[Wee, 2022] Wee, C. W. (2022). Radiotherapy for Newly Diagnosed Glioblastoma in the Elderly: What Is the Standard?. *Brain Tumor Research and Treatment*, 10(1), 12.

[White et al., 2011] White, E., Bienemann, A., Malone, J., Megraw, L., Bunnun, C., Wyatt, M., & Gill, S. (2011). An evaluation of the relationships between catheter design and tissue mechanics in achieving high-flow convection-enhanced delivery. *Journal of neuroscience methods*, 199(1), 87-97.

[Wilson et al., 2014] Wilson, T. A., Karajannis, M. A., and Harter, D. H. (2014). Glioblastoma multiforme: State of the art and future therapeutics. *Surgical Neurology International*, 5.

[Wiwatchaitawee et al., 2021] Wiwatchaitawee, K., Quarterman, J. C., Geary, S. M., & Salem, A. K. (2021). Enhancement of therapies for glioblastoma (GBM) using nanoparticle-based delivery systems. *AAPS PharmSciTech*, 22(2), 1–16.

[Wohlfart et al., 2012] Wohlfart, S., Gelperina, S., and Kreuter, J. (2012). Transport of drugs across the blood–brain barrier by nanoparticles. *Journal of Controlled Release*, 161(2):264–273. Drug Delivery Research in Europe.

[Woodworth et al., 2014] Woodworth, G. F., Dunn, G. P., Nance, E. A., Hanes, J., and Brem, H. (2014). Emerging insights into barriers to effective brain tumor therapeutics. *Frontiers in Oncology*, 4.

[Wu, 2004] Wu, L. Jiandong ding (2004). vitro degradation of three-dimensional porous poly (D, L-lactide-co-glycolide) scaffolds for tissue engineering. *Biomaterials*, 25(9200), 5821-5830.

[Xie et al., 2016] Xie, Y., Hou, W., Song, X., Yu, Y., Huang, J., Sun, X., ... & Tang, D. (2016). Ferroptosis: process and function. *Cell Death & Differentiation*, 23(3), 369-379.

[Xing et al., 2015] Xing, W. K., Shao, C., Qi, Z. Y., Yang, C., & Wang, Z. (2015). The role of Gliadel wafers in the treatment of newly diagnosed GBM: a meta-analysis. *Drug design, Development and Therapy*, 9, 3341.

[Yao et al., 2020] Yao, Y., Zhou, Y., Liu, L., Xu, Y., Chen, Q., Wang, Y., ... & Shao, A. (2020). Nanoparticle-based drug delivery in cancer therapy and its role in overcoming drug resistance. *Frontiers in Molecular Biosciences*, 7, 193.

[Yeo, Y., & Park, K.,2004) Control of encapsulation efficiency and initial burst in polymeric microparticle systems. *Archives of Pharmacal Research*, 27(1), 1-12.

[Zhang & Gao, 2007] Zhang, H., & Gao, S. (2007). Temozolomide/PLGA microparticles and antitumor activity against glioma C6 cancer cells *in vitro*. *International journal of pharmaceutics*, 329(1-2), 122-128.

[Zhang et al., 2015] Zhang, B., Yang, Y., Shi, X., Liao, W., Chen, M., Cheng, A. S. L., ... & Zou, X. (2015). Proton pump inhibitor pantoprazole abrogates adriamycin-resistant gastric cancer cell invasiveness via suppression of Akt/GSK- $\beta$ / $\beta$ -catenin signaling and epithelial–mesenchymal transition. *Cancer Letters*, 356(2), 704-712.

[Zolnik & Burgess, 2007] Zolnik, B. S., & Burgess, D. J. (2007). Effect of acidic pH on PLGA microsphere degradation and release. *Journal of Controlled Release*, 122(3), 338-344.

[Zwawi, 2021] Zwawi, M. (2021). A review on natural fiber bio-composites, surface modifications and applications. *Molecules*, 26(2), 404.